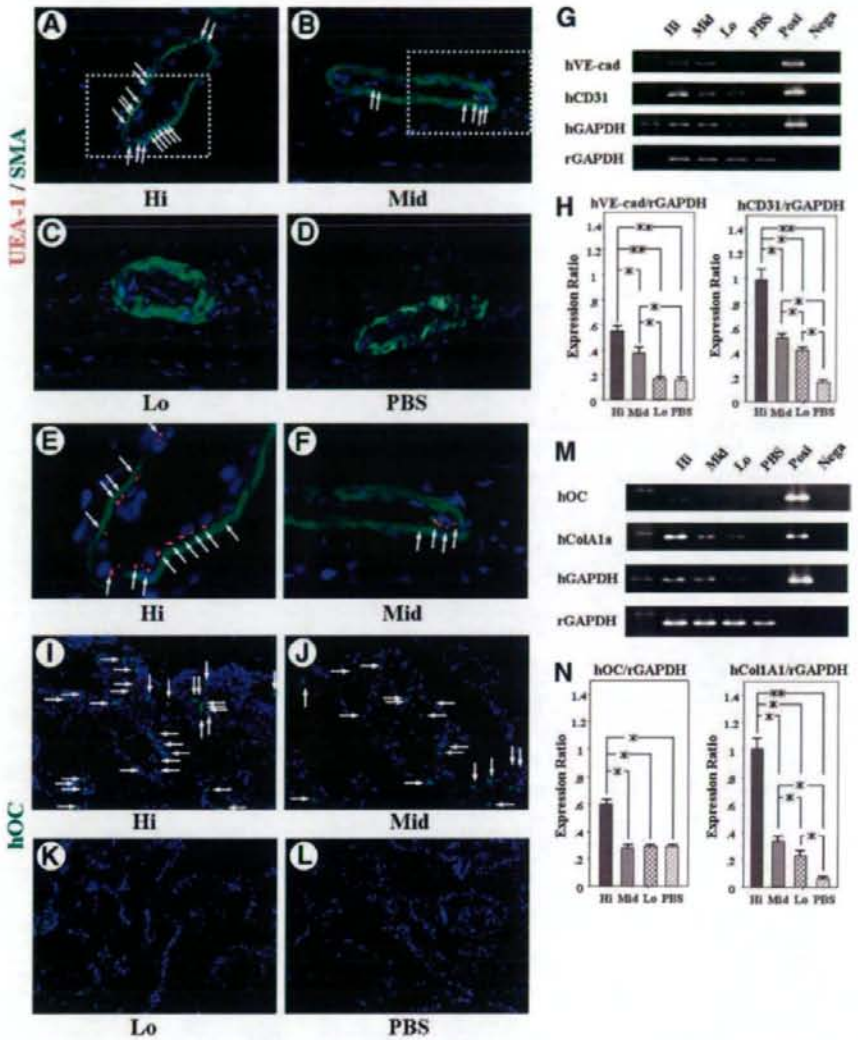

Figure 3. Fracture site vasculogenesis and osteogenesis derived from human CD34+ cells. **(A–F):** Representative double immunostaining for UEA-1 (red) and SMA (green) using tissue samples of the fracture sites at week 2 (original magnification, ×200 **[A–D]**, ×400 **[E, F]**). Differentiated human endothelial cells (ECs) identified as UEA-1 positive cells (red) were observed only in animals receiving a high dose (Hi) **(A, E)** or a middle dose (Mid) **(B, F)** of CD34+ cells but not in those treated with a low dose (Lo) **(C)** or PBS **(D)**. **(G):** Reverse transcriptase (RT) PCR analysis of tissue RNA isolated from the perifracture sites demonstrated the expression of human-specific EC markers (hVE-cad, hCD31) in animals treated with Hi, Mid, and Lo doses of CD34+ cells but not in animals receiving PBS. Cultured human umbilical vein endothelial cells were used for the Posi. For the Nega, no RNA was applied. **(H):** The ratio of gene expression of hVE-cad to rGAPDH in perifracture site was significantly greater in the Hi group than in other groups, as well as in the Mid group compared with the Lo and PBS groups. The ratio of gene expression of hCD31 to rGAPDH was significantly greater in the Hi group than in the other groups, as well as in the Mid group compared with Lo and PBS groups. **, $p < .01$; *, $p < .05$ ($n = 4$ in each group). **(I–L):** Representative immunostaining for hOC (green) using samples collected from fracture sites at week 2 (×100). Differentiated human osteoblasts (OBs) identified as hOC-positive cells (green) were observed in animals receiving Hi **(I)** and Mid **(J)** doses, but not in the Lo **(K)** and PBS **(L)** groups. **(M):** RT-PCR analysis using RNA isolated from the perifracture sites demonstrated the expression of human-specific bone-related markers (hOC and hCol1A1) in animals treated with Hi, Mid, and Lo doses of CD34+ cells but not in animals receiving PBS. Cultured human OBs were used for the Posi. **(N):** The ratio of gene expression of hOC to rGAPDH in perifracture sites was significantly greater in the Hi group than in the other groups, and the ratio of gene expression of hCol1A1 to rGAPDH was significantly greater in the Hi group than in the other groups, as well as in the Mid group compared with the Lo and PBS groups. **, $p < .01$; *, $p < .05$ ($n = 4$ in each group). Abbreviations: hGAPDH, human glyceraldehyde-3-phosphate dehydrogenase; Hi, 10^5; hOC, human-specific osteocalcin; hVE-cad, human VE-cadherin; Lo, 10^3; Mid, 10^4; Nega, negative control; PBS, phosphate-buffered saline; Posi, positive control; rGAPDH, rat glyceraldehyde-3-phosphate dehydrogenase; SMA, smooth muscle actin; UEA-1, *Ulex europaeus* lectin type 1.

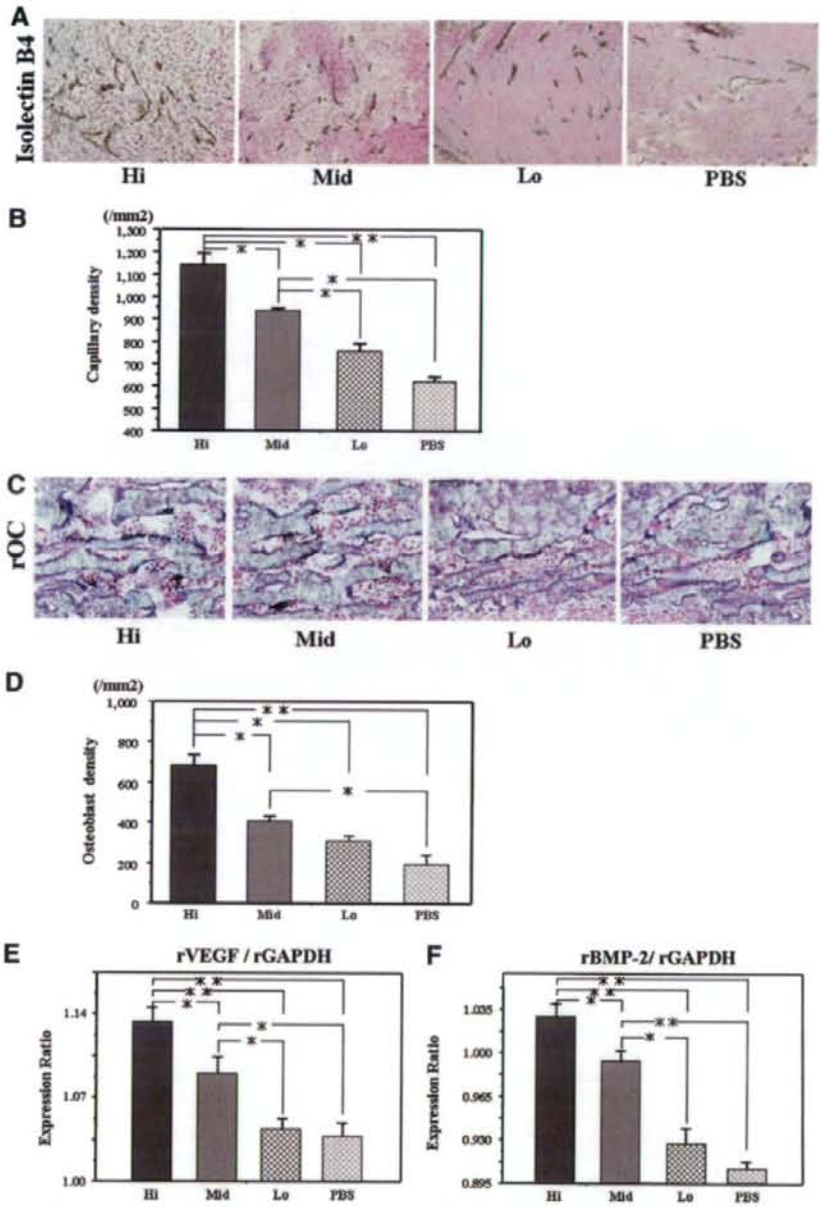

Figure 4. Enhancement of neovascularization and osteogenesis by recipient cells following granulocyte colony-stimulating factor-mobilized peripheral blood (GM-PB) CD34+ cell transplantation. **(A):** Representative vascular staining with isolectin B4 using tissue samples of perifracture sites collected at week 2 in the Hi, Mid, or Lo dose of GM-PB CD34+ cells and the PBS group (×100). **(B):** Neovascularization assessed by capillary density at week 2 was significantly greater in the Hi group than all other groups, as well as in the Mid group compared with the Lo and PBS groups. **, $p < .01$; *, $p < .05$ ($n = 4$ in each group). **(C):** Representative osteoblast staining with rOC at week 2 in animals treated with a Hi, Mid, or Lo dose of CD34+ cells or PBS alone (×200). **(D):** Osteogenesis assessed by osteoblast density at week 2 was significantly greater in the Hi group than other groups, as well as in the Mid group compared with the PBS group. **, $p < .01$; *, $p < .05$ ($n = 4$ in each group). **(E, F):** Gene expression of intrinsic cytokines for angiogenesis and osteogenesis at week 2. The mRNA expression ratio of rVEGF **(C)** and rBMP-2 **(D)** to rGAPDH at the fracture sites was significantly greater in the Hi group than other groups, as well as in the Mid group compared with the Lo and PBS groups. **, $p < .01$; *, $p < .05$ ($n = 4$ in each group). Abbreviations: Hi, 10^5; Lo, 10^3; Mid, 10^4; PBS, phosphate-buffered saline; rOC, rat osteocalcin; rBMP-2, rat bone morphogenic protein 2; rVEGF, rat vascular endothelial growth factor.

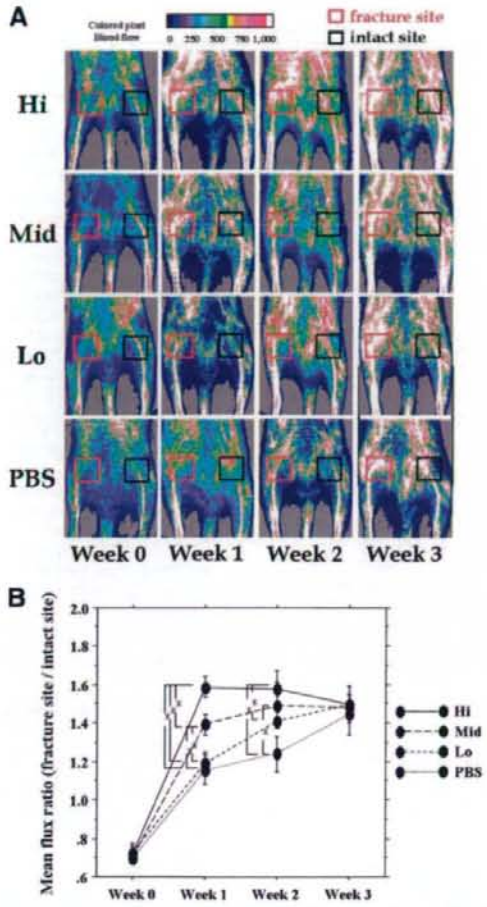

Figure 5. Improvement of blood flow at fracture sites following CD34+ cell transplantation. **(A):** Representative laser Doppler perfusion imaging (LDPI) at week 0 (1 hour after fracture), 1, 2 and 3 are shown. In these digital color-coded images, maximum perfusion values are indicated in white, medium values in green to yellow, and lowest values in dark blue. The skin blood flow within fracture site (red square) and intact contralateral site (black square) were evaluated as mean flux, and the ratio of the mean flux in the fractured site to that in the contralateral site (mean flux ratio) was calculated. **(B):** Severe reduction of the blood flow was observed 1 hour after nonhealing fracture was created (week 0) in all groups, whereas the mean flux ratio at week 1 was significantly higher in the Hi group compared with other groups, as well as in the Mid group compared with the Lo and PBS groups. At week 2, the ratio was significantly higher in the Hi group compared with the Lo and PBS groups, as well as in the Mid group compared with the PBS group. *, $p < .05$. Abbreviations: Hi, 10^5; Lo, 10^3; Mid, 10^4; PBS, phosphate-buffered saline.

Improvement of Blood Flow in Animals Receiving GM-PB CD34+ Cells After Fracture

To evaluate blood flow recovery at the fracture sites, LDPI was serially examined after fracture. LDPI analysis demonstrated severely low blood flow at the fracture site 1 hour after fracture creation (week 0) and subsequent recovery at weeks 1, 2, and 3 in all groups (Fig. 5A). In all groups, the ratio of fractured to intact (contralateral) blood flow significantly increased by week 1. There was no significant difference in the blood flow ratio of fractured to intact (contralateral) limbs 1 hour after fracture creation among any group, whereas the ratio at week 1 was significantly higher in animals receiving a high-dose of GM-PB CD34+ cells compared with the other groups, as well as in the middle-dose group compared with the low-dose and PBS groups (Hi, 1.587 ± 0.042; Mid, 1.397 ± 0.013; Lo, 1.193 ± 0.054; PBS, 1.190 ± 0.042, respectively; $p < .05$ for Hi vs. Mid, Lo, or PBS and for Mid vs. Lo or PBS group). At week 2, the blood flow ratio was still significantly higher in the Hi group compared with Lo and PBS groups, as well as in the Mid group compared with PBS group (Hi, 1.515 ± 0.035; Mid, 1.485 ± 0.015; Lo, 1.370 ± 0.040; PBS, 1.350 ± 0.020, respectively; $p < .05$ for Hi vs. Lo or PBS and for Mid vs. PBS group). At week 3, the flow ratio was similar in all groups (Hi, 1.445 ± 0.045; Mid, 1.485 ± 0.019; Lo, 1.495 ± 0.054; PBS, 1.498 ± 0.055, respectively; p = not significant) (Fig. 5B). These results indicate that local transplantation of human GM-PB CD34+ cells contributes to rapid improvement of tissue perfusion at the fracture site in a dose-dependent manner.

Morphological Fracture Healing in Animals Receiving GM-PB CD34+ Cell Transplantation

Morphological fracture healing was evaluated by radiographic and histological examinations. Thirty-three percent of animals at week 4 and all animals at week 8 that received a high-dose of CD34+ cells, as well as 11% of animals at week 4 and 50% of animals at week 8 that received a middle dose CD34+ cells, demonstrated fractures that radiographically appeared healed with bridging callus formation. Fracture sites in all animals receiving a low dose of CD34+ cells or PBS showed no bridging callus formation and subsequently displayed nonunions after 8 weeks, which is consistent with the previous reports of the natural course of this animal model [23, 24] (Fig. 6A, 6B).

Fracture healing was also histologically evaluated with toluidine blue staining. The degree of fracture healing at week 8 was assessed by the classification of Allen et al. [29] and was significantly higher in the Hi group compared with the other groups, as well as the Mid group compared with the Lo and PBS groups (Hi, 3.8 ± 0.13; Mid, 2.1 ± 0.16; Lo, 0.4 ± 0.48; PBS, 0.0 ± 0.00, respectively; $p < .01$ for Hi vs. Lo or PBS group and Mid vs. PBS group; $p < .05$ for Hi vs. Mid group and Mid vs. Lo group) (Fig. 6C, 6D). These results indicate that a nonhealing femoral fracture in a rat created by periosteal cauterization may be healed in a dose-dependent manner by local administration of human GM-PB CD34+ cells.

Discussion

Although most fractures typically heal with callus formation that bridges the fracture gap, a significant proportion (5%–10%) of fractures fail to heal and result in delayed union or persistent nonunion, caused mainly by inappropriate neoangiogenesis [30–33]. The importance of angiogenesis in bone formation/fracture healing has been noted since as early as 1763 [30], and adequate blood supply has been considered to be a key contributor to the osteogenic process [34].

In various fields of regenerative medicine, therapeutic neovascularization induced by EPC transplantation has been preclinically and even clinically tested in ischemic diseases, and promising outcomes have been reported [11–17]. Apart from potential for vasculogenic induction, adult human CD34+ cells, an EPC/hematopoietic stem cell (HSC)-enriched population, are also capable of differentiation into cardiomyocytes in vitro [35] and into cardiomyocytes and smooth muscle cells in vivo [11].

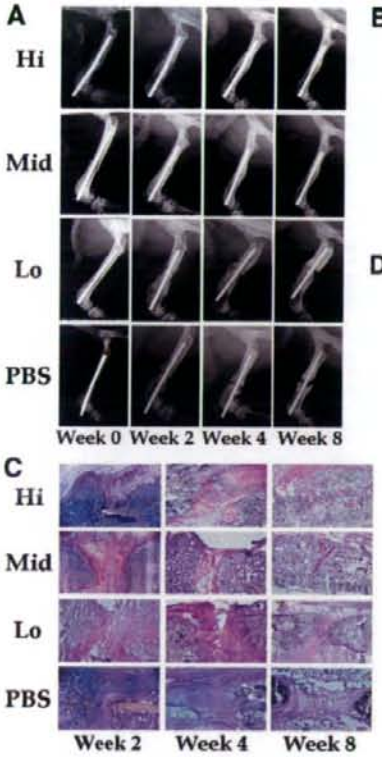

B

Period after fracture	GM-PB CD34+ cells			PBS
	High	Middle	Low	
Week 2	0/12 (0%)	0/12 (0%)	0/12 (0%)	0/12 (0%)
Week 4	3/9 (33%)	1/9 (11%)	0/9 (0%)	0/9 (0%)
Week 8	6/6* (100%)	3/6* (50%)	0/6 (0%)	0/6 (0%)

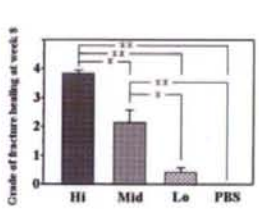

Figure 6. Radiographical and histological evidence of fracture healing following CD34+ cell transplantation. **(A):** Representative radiographs of fractured sites at weeks 0, 2, 4, and 8 in each group. **(B):** The fracture healing ratio in all groups. At week 8, in 100% of animals receiving a Hi dose of CD34+ cells and in 50% of animals receiving a Mid dose of CD34+ cells, the fracture radiographically healed with bridging callus formation. Fracture sites in all animals receiving a Lo dose of CD34+ cells or PBS showed no bridging callus formation and fell into nonunions, an outcome consistent with the previous report showing natural course of this animal model. *, $p < .05$. **(C, D):** Histological evaluation with toluidine blue staining demonstrated enhanced endochondral ossification consisting of numerous chondrocytes and newly formed trabecular bone at week 2, bridging callus formation at week 4, and complete union at week 8 in animals receiving Hi and Mid doses of CD34+ cells. In contrast, although a thick callus formation was observed at week 2, the healing process stopped by week 4, and finally the callus was absorbed at week 8 in animals receiving a Lo dose of CD34+ cells or PBS. The degree of fracture healing assessed by the classification of Allen et al. [29] was significantly higher in the Hi group than in the other groups at week 8, as well as the Mid group compared with the Lo and PBS groups. **, $p < .01$; *, $p < .05$. Abbreviations: GM-PB, granulocyte colony-stimulating factor-mobilized peripheral blood; Hi, 10^5; Lo, 10^3; Mid, 10^4; PBS, phosphate-buffered saline.

Human circulating CD133+ cells and BM CD34+ cells, both of which are EPC/HSC-enriched fractions, have been reported to differentiate into OBs in vitro [20–21]. These findings suggest that human CD34+ cells obtained from BM or PB may have the potential to differentiate into not only hematopoietic and endothelial lineages but also mesenchymal lineages, including osteogenic cells. On the basis of these studies, we previously investigated and reported the efficacy of i.v. transplantation of human circulating CD34+ cells for morphological and physiological recovery from unhealing fracture [22].

In the present study, we successfully confirmed the in vitro differentiation of human GM-PB CD34+ cells into OBs, which show matrix mineralization and calcium deposition, as well as the expression of hOC and hCol1A1 mRNA. Following our previous study, the efficacy of local transplantation of adult human GM-PB CD34+ cells was also examined in an unhealing fracture model of nude rats. To compare the incorporation efficiency between local and systemic transplantation, the human cells located in fracture sites 1 week after cell administration were detected by immunostaining for HLA-ABC. Quantification of the histological staining revealed 2.7-fold and 2.6-fold more incorporation of GM-PB CD34+ cells in the granulation area and the newly formed bone area following local transplantation with atelocollagen compared with i.v. infusion. Although homing efficiency of CD34+ cells after systemic infusion in this study was similarly impressive to that in previous reports of hind limb ischemia [14], myocardial infarction [13], and fracture [22], the cell recruitment was more efficient following local transplantation compared with systemic infusion. The result suggests that local transplantation may overcome the critical issue of CD34+ cell scarcity in clinical situations. Therefore, the effect of local transplantation of not only Hi, which was the same dose as in the previous study for i.v. infusion [22] but also Mid and Lo GM-PB CD34+ cells was examined in this study. Immunohistochemistry and RT-PCR analysis for human-specific markers revealed that direct vasculogenesis and osteogenesis by transplanted GM-PB CD34+ cells were detected in the Hi and Mid groups but not in the Lo and PBS groups. In regards to the paracrine effects of the transplanted cells on the recipient cells, immunostaining for rat-specific markers indicated significant enhancement of intrinsic angiogenesis and osteogenesis in the Hi and Mid groups but not in the other groups. We hypothesized that various cytokines and growth factors secreted from GM-PB CD34+ cells may exert a paracrine effect for intrinsic angio-osteogenesis. Endogenous vascular endothelial growth factor (VEGF) is one of the most important molecules for endochondral bone formation [36–38], and VEGF is expressed in the same temporal and spatial pattern in the fracture callus as occurs during bone development [39, 40]. VEGF activity is essential for normal angiogenesis and appropriate callus architecture and mineralization in response to bone injury [41–43]. Another growth factor, bone morphogenic protein (BMP), is also a key molecule for the process of fracture healing [44–46]. BMPs are newly synthesized by callus-forming cells near the fracture site, and BMP-2 stimulates angiogenesis via upregulation of VEGF at the fracture sites [47]. In this study, real-time RT-PCR analysis revealed overexpression of rVEGF and rBMP-2 at the perifracture sites of the Hi and Mid groups, which may be one of the mechanisms underlying the intrinsic angio-osteogenesis. Physiological assessment by LDPI showed significant recovery of blood flow at the fracture sites in the Hi and Mid groups but not in the other

groups. Finally, radiological healing of the fractures was observed only in the Hi and Mid groups. The frequency of the healing was 100% in the Hi group, 50% in the Mid group, and 0% in the Lo and PBS groups at week 8. This radiological outcome was consistent with histological evaluation of the fracture healing by the classification of Allen et al. [29]. These findings strongly suggest that local transplantation of GM-PB CD34+ cells may have the potential to repair fractures by autocrine and paracrine mechanisms of neovascularization and osteogenesis. Most importantly, the significant efficacy of the local transplantation of GM-PB CD34+ cells is found at doses equal to or more than middle dose, which is lower than the effective dose of i.v. infusion found in the previous study [22]. In contrast, transplantation of the low dose of human CD34+ cells did not significantly contribute to vasculo-osteogenesis for fracture repair. The results regarding dose effects in this preclinical study might provide helpful information for establishing a clinical strategy for this novel modality.

The mechanism of multilineage differentiation potential in human CD34+ cells into ECs and OBs is still being investigated. However, single-cell PCR assessment indicated the expression of OC in 4 of 20 CD34+ cells in our previous study [22], suggesting that direct differentiation of human CD34+ cells into OBs may contribute to the multipotent plasticity even at a low rate. Microenvironmental interaction between vascular and osteoblastic lineage cells through paracrine regulatory factors and direct cellular communications may also be involved in developing CD34+ cells and may be conducive to fracture healing. We speculate that an enhanced vasculogenesis signal may cause the cellular commitment and development of CD34+ cells into osteoblastic cells as a cooperative organogenesis mechanism.

Several research groups have demonstrated the usefulness of local transplantation of total BM cells for fracture healing [48–51]. Hernigou et al. reported that in 88% of patients with noninfected nonunions of the tibia, bone union was achieved by percutaneous grafting of autologous total BM cells accompanied by external fixation or cast immobilization [51]. Compared with transplantation of purified CD34+ cells, total BM cell transplantation does not require a magnetic cell sorting process, indicating that time and cost of the cell preparation can be diminished. However, our group recently reported that intramyocardial transplantation of human GM-PB total MNCs represents a possible risk of severe hemorrhagic myocardial infarction in nude rats through the excessive inflammation induced by abundant infiltration of hematopoietic cells [52]. Thus, additional preclinical/clinical studies would be warranted to compare the feasibility, safety, and efficacy of both strategies for bone repair.

Concerning future clinical application, the biological risk of G-CSF may also become a problem. G-CSF has been used in thousands of clinical cases; however, severe complications, such as spleen rupture, interstitial pneumonitis, and acute coronary syndrome, are rarely reported [53]. This rare but potential risk of G-CSF, as well as the high cost of CD34+ cell isolation, would need to be overcome in the future.

Conclusion

In conclusion, the present findings suggest that local transplantation of GM-PB CD34+ cells could be a promising clinical strategy for enhancing bone repair in patients suffering from unhealing fracture.

Disclosure of Potential Conflicts of Interest

The authors indicate no potential conflicts of interest.

References

1 Blau HM, Brazelton TR, Weimann JM. The evolving concept of a stem cell: Entity or function? Cell 2001;105:829–841.
2 Korbling M, Estrov Z. Adult stem cells for tissue repair: A new therapeutic concept? N Engl J Med 2003;349:570–582.
3 Slack JM. Stem cells in epithelial tissues. Science 2000;287:1431–1433.
4 Pardanaud L, Yassine F, Dieterlen-Lievre F. Relationship between vasculogenesis, angiogenesis and haemopoiesis during avian ontogeny. Development 1989;105:473–485.
5 Risau W, Sariola H, Zerwes HG et al. Vasculogenesis and angiogenesis in embryonic-stem-cell-derived embryoid bodies. Development 1988; 102:471–478.
6 Asahara T, Murohara T, Sullivan A et al. Isolation of putative progenitor endothelial cells for angiogenesis. Science 1997;275:964–967.
7 Asahara T, Masuda H, Takahashi T et al. Bone marrow origin of endothelial progenitor cells responsible for postnatal vasculogenesis in physiological and pathological neovascularization. Circ Res 1999;85: 221–228.
8 Takahashi T, Kalka C, Masuda H et al. Ischemia- and cytokine-induced mobilization of bone marrow-derived endothelial progenitor cells for neovascularization. Nat Med 1999;5:434–438.
9 Assmus B, Schachinger V, Teupe C et al. Transplantation of progenitor cells and regeneration enhancement in acute myocardial infarction (TOPCARE-AMI). Circulation 2002;106:3009–3017.
10 Britten MB, Abolmaali ND, Assmus B et al. Infarct remodeling after intracoronary progenitor cell treatment in patients with acute myocardial infarction (TOPCARE-AMI): Mechanistic insights from serial contrast-enhanced magnetic resonance imaging. Circulation 2003;108:2212–2218.
11 Iwasaki H, Kawamoto A, Ishikawa M et al. Dose-dependent contribution of CD34-positive cell transplantation to concurrent vasculogenesis and cardiomyogenesis for functional regenerative recovery after myocardial infarction. Circulation 2006;113:1311–1325.
12 Kawamoto A, Gwon HC, Iwaguro H et al. Therapeutic potential of ex vivo expanded endothelial progenitor cells for myocardial ischemia. Circulation 2001;103:634–637.
13 Kawamoto A, Tkebuchava T, Yamaguchi J et al. Intramyocardial transplantation of autologous endothelial progenitor cells for therapeutic neovascularization of myocardial ischemia. Circulation 2003; 107:461–468.
14 Kalka C, Masuda H, Takahashi T et al. Transplantation of ex vivo expanded endothelial progenitor cells for therapeutic neovascularization. Proc Natl Acad Sci U S A 2000;97:3422–3427.
15 Murohara T, Ikeda H, Duan J et al. Transplanted cord blood-derived endothelial precursor cells augment postnatal neovascularization. J Clin Invest 2000;105:1527–1536.
16 Werner N, Junk S, Laufs U et al. Intravenous transfusion of endothelial progenitor cells reduces neointima formation after vascular injury. Circ Res 2003;93:e17–e24.
17 Taguchi A, Soma T, Tanaka H et al. Administration of CD34+ cells after stroke enhances neurogenesis via angiogenesis in a mouse model. J Clin Invest 2004;114:330–338.
18 Sivan-Loukianova E, Awad OA, Stepanovic V et al. CD34+ blood cells accelerate vascularization and healing of diabetic mouse skin wounds. J Vasc Res 2003;40:368–377.
19 Eghbali-Fatourechi GZ, Lamsam J, Fraser D et al. Circulating osteoblast-lineage cells in humans. N Engl J Med 2005;352:1959–1966.
20 Chen JL, Hunt P, McElvain M et al. Osteoblast precursor cells are found in CD34+ cells from human bone marrow. STEM CELLS 1997;15:368–377.
21 Tondreau T, Meuleman N, Delforge A et al. Mesenchymal stem cells derive from CD133 positive cells in mobilized peripheral blood and cord blood: Proliferation, Oct-4 expression and plasticity STEM CELLS 2005; 23:1105–1112.
22 Matsumoto T, Kawamoto A, Kuroda R et al. Therapeutic potential of vasculogenesis and osteogenesis promoted by peripheral blood CD34-positive cells for functional bone healing. Am J Pathol 2006;169: 1440–1457.
23 Einhorn TA. Enhancement of fracture-healing. J Bone Joint Surg Am 1995;77:940–956.
24 Kokubu T, Hak DJ, Hazelwood SJ et al. Development of an atrophic

nonunion model and comparison to a closed healing fracture in rat femur. J Orthop Res 2003;21:503–510.
25 Hisatome T, Yasunaga Y, Yanada S et al. Neovascularization and bone regeneration by implantation of autologous bone marrow mononuclear cells. Biomaterials 2005;26:4550–4556.
26 Ito Y, Ochi M, Adachi N et al. Repair of osteochondral defect with tissue-engineered chondral plug in a rabbit model. Arthroscopy 2005;21: 1155–1163.
27 Linden M, Sirsjo A, Lindbom L et al. Laser-Doppler perfusion imaging of microvascular blood flow in rabbit tenuissimus muscle. Am J Physiology 2005;269:H1496–H1500.
28 Wardell K, Jakobsson A, Nilsson GE. IEEE laser Doppler perfusion imaging by dynamic light scattering. IEEE Trans Biomed Eng 1993;40: 309–316.
29 Allen HL, Wase A, Bear WT. Indomethacin and aspirin: Effect of nonsteroidal anti-inflammatory agents on the rate of fracture repair in the rat. Acta Orthop Scand 1980;51:595–600.
30 Colnot CI, Helms JA. A molecular analysis of matrix remodeling and angiogenesis during long bone development. Mech Dev 2001;100: 245–250.
31 Gerstenfeld LC, Cullinane DM, Barnes GL, et al. Fracture healing as a post-natal developmental process: Molecular, spatial, and temporal aspects of its regulation. J Cell Biochem 2003;88:873–884.
32 Marsh D. Concepts of fracture union, delayed union, and nonunion. Clin Orthop Relat Res 1998:S22–S30.
33 Rodriguez-Merchan EC, Forriol F. Nonunion: General principles and experimental data. Clin Orthop Relat Res 2004:4–12.
34 Burkhardt R, Kettner G, Bohm W et al. Changes in trabecular bone, hematopoiesis and bone marrow vessels in aplastic anemia, primary osteoporosis, and old age: A comparative histomorphometric study. Bone 1987;8:157–164.
35 Badorff C, Brandes RP, Popp R et al. Transdifferentiation of blood-derived human adult endothelial progenitor cells into functionally active cardiomyocytes. Circulation 2003;107:1024–1032.
36 Zelzer E, McLean W, Ng YS et al. Skeletal defects in VEGF(120/120) mice reveal multiple roles for VEGF in skeletogenesis. Development 2002;129:1893–1904.
37 Haigh JJ, Gerber HP, Ferrara N et al. Conditional inactivation of VEGF-A in areas of collagen2a1 expression results in embryonic lethality in the heterozygous state. Development 2000;127:1445–1453.
38 Gerber HP, Vu TH, Ryan AM et al. VEGF couples hypertrophic cartilage remodeling, ossification and angiogenesis during endochondral bone formation. Nat Med 1999;5:623–628.
39 Ferguson C, Alpern E, Miclau T et al. Does adult fracture repair recapitulate embryonic skeletal formation? Mech Dev 1999;87:57–66.
40 Ryan AM, Eppler DB, Hagler KE et al. Preclinical safety evaluation of rhuMAbVEGF, an antiangiogenic humanized monoclonal antibody. Toxicol Pathol 1999;27:78–86.
41 Peng H, Wright V, Usas A et al. Synergistic enhancement of bone formation and healing by stem cell-expressed VEGF and bone morphogenetic protein-4. J Clin Invest 2002;110:751–759.
42 Street J, Bao M, deGuzman L et al. Vascular endothelial growth factor stimulates bone repair by promoting angiogenesis and bone turnover. Proc Natl Acad Sci U S A 2002;99:9656–9661.
43 Tatsuyama K, Maezawa Y, Baba H et al. Expression of various growth factors for cell proliferation and cytodifferentiation during fracture repair of bone. Eur J Histochem 2000;44:269–278.
44 Bostrom MP, Lane JM, Berberian WS et al. Immunolocalization and expression of bone morphogenetic proteins 2 and 4 in fracture healing. J Orthop Res 1995;13:357–367.
45 Meyer RA Jr, Meyer MH, Tenholder M et al. Gene expression in older rats with delayed union of femoral fractures. J Bone Joint Surg Am 2003;85A:1243–1254.
46 Onishi T, Ishidou Y, Nagamine T et al. Distinct and overlapping patterns of localization of bone morphogenetic protein (BMP) family members and a BMP type II receptor during fracture healing in rats. Bone 1998; 22:605–612.
47 Deckers MM, van Bezooijen RL, van der Horst G et al. Bone morphogenetic proteins stimulate angiogenesis through osteoblast-derived vascular endothelial growth factor A. Endocrinology 2002;143:1545–1553.
48 Healey JH, Zimmerman PA, McDonnell JM et al. Percutaneous bone marrow grafting of delayed union and nonunion in cancer patients. Clin Orthop Relat Res 1990:280–285.
49 Connolly JF, Guse R, Tiedeman J et al. Autologous marrow injection as a substitute for operative grafting of tibial nonunions. Clin Orthop Relat Res 1991:259–270.
50 Garg NK, Gaur S, Sharma S. Percutaneous autogenous bone marrow grafting in 20 cases of ununited fracture. Acta Orthop Scand 1993;64: 671–672.
51 Hernigou P, Poignard A, Beaujean F et al. Percutaneous autologous bone-marrow grafting for nonunions. Influence of the number and concentration of progenitor cells. J Bone Joint Surg Am 2005;87: 1430–1437.
52 Kawamoto A, Iwasaki H, Kusano K et al. CD34-positive cells exhibit increased potency and safety for therapeutic neovascularization after myocardial infarction compared with total mononuclear cells. Circulation 2006;114:2163–2169.
53 Becker PS, Wagle M, Matous S et al. Spontaneous splenic rupture following administration of granulocyte colony-stimulating factor (G-CSF): Occurrence in an allogeneic donor of peripheral blood stem cells. Biol Blood Marrow Transplant 1997;3:45–49.

See www.StemCells.com for supplemental material available online.

STEM CELLS
TRANSLATIONAL AND CLINICAL RESEARCH

Administrations of Peripheral Blood CD34-Positive Cells Contribute to Medial Collateral Ligament Healing via Vasculogenesis

KATSUMASA TEI,[a] TOMOYUKI MATSUMOTO,[a,b] YUTAKA MIFUNE,[a,b] KAZUNARI ISHIDA,[a] KEN SASAKI,[a] TARO SHOJI,[a,b] SEIJI KUBO,[a] ATSUHIKO KAWAMOTO,[b] TAKAYUKI ASAHARA,[b,c] MASAHIRO KUROSAKA,[a] RYOSUKE KURODA[a]

[a]Department of Orthopedic Surgery, Kobe University Graduate School of Medicine, Kobe, Japan; [b]Stem Cell Translational Research, Kobe Institute of Biomedical Research and Innovation, RIKEN Center for Developmental Biology, Kobe, Japan; [c]Department of Regenerative Medicine Science, Tokai University School of Medicine, Isehara, Kanagawa, Japan

Key Words. Endothelial progenitor cells • Vascularization • Ligament healing

ABSTRACT

Neoangiogenesis is a key process in the initial phase of ligament healing. Adult human circulating CD34+ cells, an endothelial/hematopoietic progenitor-enriched cell population, have been reported to contribute to neoangiogenesis; however, the therapeutic potential of CD34+ cells for ligament healing is still unclear. Therefore, we performed a series of experiments to test our hypothesis that ligament healing is supported by CD34+ cells via vasculogenesis. Granulocyte colony-stimulating factor-mobilized peripheral blood (GM-PB) CD34+ cells with atelocollagen (CD34+ group), GM-PB mononuclear cells (MNCs) with atelocollagen (MNC group), or atelocollagen alone (control group) was locally transplanted after the creation of medial collateral ligament injury in immunodeficient rats. Reverse transcriptase-polymerase chain reaction (RT-PCR) and immunohistochemical staining at the injury site demonstrated that molecular and histological expression of human-specific markers for endothelial cells was higher in the CD34+ group compared with the other groups at week 1. Endogenous effect, assessed by capillary density and mRNA expression of vascular endothelial growth factor, was significantly higher in CD34+ cell group than the other groups. In addition to the observation that, as assessed by real-time RT-PCR, gene expression of ligament-specific marker was significantly higher in the CD34+ group than in the other groups, ligament healing assessed by macroscopic, histological, and biomechanical examination was significantly enhanced by CD34+ cell transplantation compared with the other groups. Our data strongly suggest that local transplantation of circulating human CD34+ cells may augment the ligament healing process by promoting a favorable environment through neovascularization. STEM CELLS *2008;26:819–830*

Disclosure of potential conflicts of interest is found at the end of this article.

INTRODUCTION

Ligaments, made of dense connective parallel tissue fibers, play an essential role in mediating normal movement and stability of joints. Injury to these systems causes significant joint instability, which may lead to injury of other tissues and the development of degenerative joint disease. In most cases, such as anterior cruciate ligament injury, healing fails to take place, and replacement tissues or grafts are required. However, it has been reported that the mechanical properties of the healing ligament do not return to normal 1 year after injury in both rabbit and canine models [1, 2]. Although use of cells such as cultured fibroblasts, myoblasts, or mesenchymal stem cells as a biological vehicle [3–5] or use of some growth factors [6–11] results in some success, a more in-depth analysis of the cellular and molecular mechanisms in ligament healing may offer novel opportunities for the development of new therapies for patients with ligament injuries.

The serial stages of ligament healing are well understood as cellular processes. Following the initial hemorrhagic reaction, multiple cell types recruit to the wound while the granulation tissue is formed [12, 13]. In this process, neovascularization is recognized as a crucial initiator of ligament healing and remodeling [13]. However, it is still unclear which types of cells contribute to the development of ligament healing and how the neovascularization process originates and is enhanced. Vasculogenesis by endothelial progenitor cells (EPCs), which is involved in the development of the blood vessel system in the embryonic stage [12, 14], was not identified as a mechanism of postnatal endothelial regeneration until the discovery of bone marrow (BM)-derived and circulating EPCs in adults [15–17]. As a result of this finding, many researchers have applied EPCs for therapeutic neovascularization and acquired beneficial results for limb ischemia, myocardial infarction, stroke, and diabetic wounds in animal models [18–29]. Following these promising reports, we quite recently reported that human CD34+ cell transplantation induced significant vasculogenesis in regenerating tissues and enhanced functional recovery from nonhealing fractures in small animal models [30]. Although those beneficial results via vasculogenesis/angiogenesis for various diseases have been reported, the efficacy and role of circulating CD34+ cells for ligament healing have not been clarified. Therefore, we tested the hypothesis that transplantation of circulating

Correspondence: Ryosuke Kuroda, M.D., Ph.D., Department of Orthopaedic Surgery, Kobe University Graduate School of Medicine 7-5-1, Kusunoki-cho, Chuo-ku, Kobe, 650-0017, Japan. Telephone: 81-78-382-5985; Fax: 81-78-351-6930; e-mail: kurodar@med.kobe-u.ac.jp Received August 23, 2007; accepted for publication December 25, 2007; first published online in STEM CELLS *EXPRESS* January 10, 2008. 1066-5099/2008/$30.00/0 doi: 10.1634/stemcells.2007-0671

CD34+ cells may contribute to ligament healing via vasculogenesis/angiogenesis.

In the present series of experiments, we demonstrated that human circulating CD34+ cells, locally transplanted with atelocollagen, survived at the injury site of the medial collateral ligament (MCL) injury in an immunodeficient rat model, developed a favorable environment for ligament healing by enhancing vasculogenesis and angiogenesis, and finally led to functional recovery from injury. The present findings have important clinical implications for cell-based therapy that will enhance ligament repair following injury.

MATERIALS AND METHODS

Preparation of Human Cells

We purchased frozen human granulocyte-stimulating factor-mobilized peripheral blood (GM-PB) CD34+ cells obtained from healthy black females (43 and 28 years old) and frozen human GM-PB mononuclear cells (MNCs) obtained from healthy black females (25 and 38 years old) from Cambrex (Walkersville, MD, http://www.cambrex.com). We thawed out the cells for experimental use according to the manuals from Cambrex.

Flow Cytometry Studies and Monoclonal Antibodies

Regular flow cytometric profiles of GM-PB CD34+ cells and GM-PB MNCs were analyzed with a FACSCalibur analyzer and CellQuest software (Becton, Dickinson Immunocytometry Systems, Mountain View, CA, http://www.bd.com). The procedure was described previously [20, 30]. The following monoclonal antibodies were used to characterize the CD34+ cell population: CD34-APC (BD Pharmingen, San Diego, http://www.bdbiosciences.com/index_us.shtml), CD34-fluorescein isothiocyanate (FITC) (BD Pharmingen), CD45-APC (BD Pharmingen), CD133-APC (BD Pharmingen), c-Kit-PE (Nichirei, Tokyo, http://www.nichirei.co.jp/english/index.html), CD31-PE (BD Pharmingen), IgG1-FITC isotype controls (BD Pharmingen), IgG1-APC isotype controls (BD Pharmingen), and PI (Sigma-Aldrich, St. Louis, http://www.sigmaaldrich.com).

Induction of MCL Injury and Cell Transplantation

Female athymic nude rats (F344/N Jcl rnu/rnu; CLEA Japan, Tokyo, http://www.clea-japan.com) ages 8–12 weeks and weighing 150–170 g were used in this study. The rats were fed a standard maintenance diet and provided with water ad libitum. The institutional animal care and use committees of Kobe University approved all animal procedures, including human cell transplantation.

All surgical procedures were performed under anesthesia and normal sterile conditions. Anesthesia was performed with ketamine hydrochloride (60 mg/kg) and xylazine hydrochloride (10 mg/kg) administered intraperitoneally. The surgical procedure was performed according to the method of Watanabe et al. [31]. Briefly, the right knee joint was approached through a medial skin incision, and the MCL of rat was cut transversely, together with the fascia covering the MCL, using a microsurgical technique. Next, the fascia was sutured, and the fascial pocket was made to maintain the transplanted cells with 200 μl of atelocollagen gel (2% solution; pH 7.3; osmolality, 260 mOsm/kgH_2O; Koken, Tokyo, http://www.kokenmpc.co.jp/english) in the healing site. Human GM-PB CD34+ cells (1×10^5; Cambrex) were transplanted with atelocollagen in the right knee (CD34+ group), and atelocollagen without cells was transplanted in the left knee as a control group ($n = 32$). On the other hand, 1×10^5 GM-PB MNCs (Cambrex) were transplanted with atelocollagen as a cellular control group in the right knee (MNC group), and a bolus of atelocollagen without cells was transplanted in the left knee as a control group ($n = 32$). Atelocollagen gel was chosen as a cell carrier because of its immunogenic and safety advantages over other carriers. Atelocollagen solution is in liquid form when cooled to 4°C and adjusted to neural pH but gelatinizes as the temperature rises to 37°C. In atelocollagen, the antigenic telopeptide region is removed by pepsin digestion and differential salt precipitation during purification. This immunogenic advantage has enabled atelocollagen to be used in various clinical settings. Transplantations were done immediately after mixture of the appropriately medium-suspended cells and atelocollagen gel or mixture of the same bolus of medium and atelocollagen. These atelocollagen procedures were reported previously [32, 33]. Thirty-two left knees were randomly selected from 64 samples in the control group for this study.

Six rats for macroscopic and histological assessment and six rats for biomechanical assessment were randomly selected from each group and sacrificed at weeks 2 and 4. Five rats for immunohistochemistry and three rats for reverse transcriptase-polymerase chain reaction (RT-PCR) were also randomly selected from each group and sacrificed at week 1. If the MCL injury was not a stable transverse injury or if any evidence of deep infection was seen, the animals were excluded from the study and replaced with additional animals. Thus, two rats with comminuted injury were replaced during the experiment; however, no rats with infection macroscopically were replaced.

RT-PCR Analysis of RNA Isolated from GM-PB CD34+ Cells and Peri-injury Site Tissue of MCL

Total RNA was obtained from human GM-PB CD34+ cells and the rat tissues at the in peri-injury site of MCL at week 1 ($n = 3$) using Tri-zol (Life Technologies, Rockville, MD, http://www.lifetech.com) according to the manufacturer's instructions. This procedure was described previously [20, 30].

To avoid interspecies cross-reactivity of the primer pairs between human and rat genes, we designed the following human(h)-specific primers using Oligo software (Takara, Otsu, Japan, http://www.takara.co.jp). No primer pairs showed cross-reactivity to rat genes (data not shown).

Human (h) CD34 primer sequence (380 base pairs [bp]): sense, AAT GAG GCC ACA ACA AAC ATC ACA; antisense, CTG TCC TTC TTA ACC TCC GCA CAG C;
hCD31 primer sequence (363 bp): sense, ATC GAT CAG TGG AAC TTT GCC TAT T; antisense, GTG GCA TTT GAG ATT TGA TAG A;
Human vascular endothelial-cadherin (hVE-Cad) primer sequence (461 bp): sense, ACG CCT CTG TCA TGT ACC AAA TCC T; antisense, GGC CTC GAC GAT GAA GCT GTA TT;
Human vascular endothelial growth factor (hVEGF) primer sequence (235 bp): sense, ATG GCA GAA GGA GGG CAG CAT; antisense, TTG GTG AGG TTT GAT CCG CAT CAT;
Human hepatocyte growth factor (hHGF) primer sequence (423 bp): sense, ATG CTC ATG GAC CCT GGT; antisense, GCC TGG CAA GCT TCA TTA;
Human kinase insert domain-containing receptor (hKDR) primer sequence (468 bp): sense, CAA ATG TGA AGC GGT CAA CAA AGT T; antisense, ATG CTT TCC CCA ATA CTT GTC GTC T;
hCD45 primer sequence (312 bp): sense, CAC TGC AGG GAT GGA TCT CA; antisense, ACT CGT GGG TTC AGA ACC TTC A;
hCD11b primer sequence (409 bp): sense, GAG TAC GTG CCA CAC CAA GGA; antisense, GAC CCC CTT CAC TCA TCA TGT CT;
hCD14 primer sequence (361 bp): sense, TCC GAA GCC TTC CAG TGT GT; antisense, TTG GGC AAT GCT CAG TAC CTT;
Human glyceraldehyde-3-phosphate dehydrogenase (hGAPDH) primer sequence (596 bp): sense, CTG ATG CCC CCA TGT TCG TC; antisense, CAC CCT GTT GCT GTA GCC AAA TTC G;
Rat glyceraldehyde-3-phosphate dehydrogenase (rGAPDH) primer sequence (320 bp): sense, GTG CCA GCC TCG TCT CAT AGA; antisense, CGC CAG TAG ACT CCA CGA CAT.

Real-Time RT-PCR Analysis of Recipients' Cytokines in the Peri-injury Site Tissue of MCL

Total RNA was obtained from the rat tissues at the peri-injury site 1 week after surgery by the same methods as RT-PCR. Following total RNA isolation, the converted cDNA (2 μl) samples were amplified in triplicate by real-time PCR (ABI PRISM 7700; Applied Biosystems, Foster City, CA, http://www.appliedbiosystems.com) at a final volume of 20 μl using SYBR Green Master Mix

(Applied Biosystems) reagent at a final concentration of 1×. Melting curve analysis was performed using Dissociation Curves software (Applied Biosystems) to ensure that only a single product was amplified. Specificity of the reactions was confirmed by 2.0% agarose gel electrophoresis. Results were obtained using sequence detection software (ABI PRISM 7700; Applied Biosystems) and evaluated using Microsoft Excel (Redmond, WA, http://www.microsoft.com).

Primers were as follows.

Rat vascular endothelial growth factor (rVEGF) primer sequence (253 bp): sense, AAG CAA GTA GCG CCA ATC T; antisense, GGA AGT AGG GTG CCA TAA CAC;
Rat tenomodulin (rTeM) primer sequence (71 bp): sense, CCA TGC TGG ATG AGA GAG GTT AC; antisense, CAC AGA CCC TGC GGC AGT A;
Rat collagen1A2 (rCol1A2) primer sequence (67 bp): sense, GCT TTG TGG ATA CGC GAA CTC; antisense, CCA GCA TTG GCA TGT TGC T;
rGAPDH primer sequence (67 bp): sense, TGC CAT CAC TGC CAC TCA GA; antisense, CCC CAC GGC CAT CAC A.

Tissue Harvesting

Rats were euthanized with an overdose of ketamine and xylazine. Bilateral knees were harvested and quickly embedded in optimal cutting temperature (OCT) compound (Sakura Finetek, Torrance, CA, http://www.sakura.com), snap-frozen in liquid nitrogen, and stored at −80°C for histological, histochemical, and immunohistochemical staining as described below. Rat knees in OCT blocks were sectioned, and 6-μm serial sections were mounted on silane-coated glass slides and air-dried for 1 hour before being fixed with 4.0% paraformaldehyde at 4°C for 5 minutes and stained immediately.

Immunofluorescent Staining

To detect transplanted human cells in the rat injury site of MCL, immunohistochemistry (n = 5 in each group) was performed at week 1 with following human-specific antibodies: human nuclei antibody (HNA) (Chemicon, Temecula, CA, http://www.chemicon.com), human leukocyte antigen (HLA)-ABC (BD Pharmingen) to detect various kind of human cells, human-specific *Ulex europaeus* lectin type 1 (UEA-1) (Vector Laboratories, Burlingame, CA, http://www.vectorlabs.com) to detect human endothelial cells (ECs), and human-specific CD45 (BD Biosciences, San Diego, http://www.bdbiosciences.com) to detect human hematopoietic/inflammatory cells. Staining specificity for human cells without cross-reaction to rat cells was confirmed by histochemical staining for HNA, HLA-ABC, UEA-1, and CD45 using human and rat heart (data not shown). Double immunohistochemistry with HNA and smooth muscle actin (SMA) was performed to detect various surviving human cells in the arterioles. Double immunohistochemistry with HLA-ABC and UEA-1 was also performed to distinguish differentiation of transplanted CD34+ cells into ECs and the other various kind of human cells. The secondary antibodies for each immunostaining were as follows: Cy3-conjugated streptavidin (Jackson Immunoresearch Laboratories, West Grove, PA, http://www.jacksonimmuno.com) for UEA-1 staining, Alexa Fluor 594-conjugated goat anti-mouse IgG_1 (Molecular Probes, Eugene, OR, http://probes.invitrogen.com) for HNA, and Alexa Fluor 488-conjugated goat anti-mouse IgG_{2a} (Molecular Probes) for SMA and HLA-ABC. 4,6-Diamidino-2-phenylindole (DAPI) solution was applied for 5 minutes for nuclear staining.

Morphometric Evaluation of Capillary Density

Immunohistochemical staining (n = 5 in each group) for isolectin B4 (Vector Laboratories) as a rat EC marker at week 2 was visualized with fluorescence, and capillary density was morphometrically evaluated as the average value in five randomly selected fields (250 × 250 μm) of soft tissue at the peri-injury site (Fig. 3A). Capillaries were recognized as tubular structures positive for isolectin B4. All morphometric studies were performed by two examiners blind to treatment.

Macroscopic Assessment of the MCL Healing

In six of the knees from each group euthanized at 2 and 4 weeks after surgery, the MCLs were carefully identified, and the cut portions of ligament were inspected macroscopically. MCL healing was defined by the presence of bridged fibrous continuity between cut ligament edges. Macroscopes of each animal were examined by three observers blind to treatment.

Histological Assessment of the MCL Healing

Histological evaluation (n = 6 in each group) was performed with hematoxylin and eosin (HE) staining to address the process of ligament healing at weeks 2 and 4. All morphometric studies were performed by two orthopedic surgeons blind to treatment.

Biomechanical Testing

At weeks 2 and 4, six rats in each group were used for biomechanical evaluation. The hind limbs were wrapped in gauze soaked in saline solution and frozen at −20°C for later testing. Before biomechanical testing, the hind limbs were gradually thawed at room temperature, and all soft tissue spanning the knee, except for the MCL, was sharply transected. The femur-MCL-tibia complex was mounted in a specially designed device using acrylic resin, and fixed in a mechanical testing machine (Autograph AGS-5kNG; Shimadzu Corp., Kyoto, Japan, http://www.shimadzu.com/). The femur and tibia were oriented at angles of 60° and 0° from the loading axis, respectively, so that the load was directed along the longitudinal axis of the MCL. A tensile load was then applied at a rate of 0.25 mm/second until gross failure of the MCL occurred. During the tensile testing, the load-deformation relationship was recorded using a computer analysis system. The ultimate load (peak of curve) was calculated from the load-deformation curve. In addition to the tensile tests on the healing ligaments, mechanical tests were also performed on a sham-exposed MCL to obtain normal control values. The four normal, uninjured ligaments were prepared, tested, and measured in the same way as the experimental specimens.

Inhibition of Neovascularization

To investigate the hypothesis that neovascularization is essential for supporting endogenous ligament healing, we used an antiangiogenic agent, soluble Flt1 (sFlt1) (vascular endothelial growth factor [VEGF] receptor 1), known to inhibit proliferation of ECs. Rats subjected to MCL injury and CD34+ cell transplantation were divided into two groups, one group receiving sFlt1 (20 μg/kg, subcutaneous; R&D Systems Inc., Minneapolis, http://www.rndsystems.com) once daily for 14 days and the other receiving phosphate-buffered saline (PBS) only (n = 12 in each group). On week 2 (n = 6 in each group) and week 4 (n = 6 in each group) after cell transplantation, macroscopic, histological, and immunohistological assessments were performed in each group.

Statistical Analysis

All values are expressed as mean ± SE. The comparisons among three groups were made using one-way analysis of variance. Post hoc analysis was performed by Fisher's PLSD test. A probability value <0.05 was considered to denote statistical significance.

RESULTS

Phenotypic Characterization of GM-PB CD34+ Cells and GM-PB MNCs

We prepared GM-PB CD34+ cells and GM-PB MNCs from healthy males (Cambrex). The CD34+ cell fraction had a purity of >99% in GM-PB CD34+ cells (Fig. 1A) and approximately 2% in GM-PB MNCs (Fig. 1B), as determined by fluorescence-activated cell sorting (FACS) analysis to be positive for cell surface markers of CD133, CD31, CD45, and c-Kit (Fig. 1C, 1D). RT-PCR analysis of the GM-PB CD34+ cells revealed

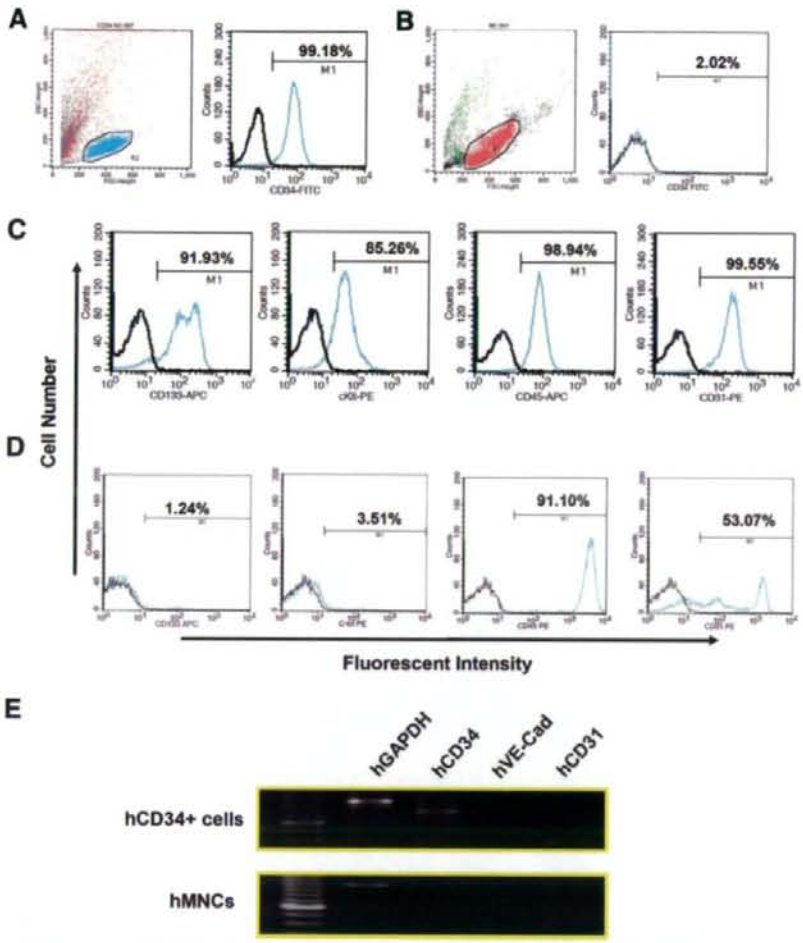

Figure 1. Phenotypic characterization of granulocyte colony-stimulating factor-mobilized peripheral blood (GM-PB) CD34+ cells and GM-PB mononuclear cells (MNCs). **(A):** The left plotting graph demonstrates that R2 gated cells with the physical properties of lymphomonocytic cells are instead included in the subsequent analyses in GM-PB CD34+ cells. The right graph demonstrates that GM-PB CD34+ cell fraction had a purity of >99%. The black line represents isotype control (negative control), and the blue line indicates sample data. The *x*-axis shows fluorescent intensity of cells, and the *y*-axis demonstrates the number of cells. **(B):** The left plotting graph demonstrates that R2 gated cells with the physical properties of lymphomonocytic cells are instead included in the subsequent analyses in GM-PB MNCs. The right graph demonstrates that the CD34+ cell fraction had a purity of approximately 2% in GM-PB MNCs. **(C):** GM-PB CD34+ cells were characterized by fluorescence-activated cell sorting analysis to be positive for the cell surface markers CD133, CD31, CD45, and c-Kit. **(D):** GM-PB MNCs were characterized as in **(C)**. **(E):** Reverse transcription-polymerase chain reaction analysis of GM-PB CD34+ cells revealed weak expression of the hCD31 but not of the other endothelial marker (hVE-Cad), whereas GM-PB MNCs revealed very weak expression of the hCD31 gene, but not of hVE-Cad and not, for the most part, of hCD34. Abbreviations: FITC, fluorescein isothiocyanate; hCD31, human-specific CD31 gene; hCD34, human CD34; hGAPDH, human glyceraldehyde-3-phosphate dehydrogenase; hMNC, human mononuclear cell; hVE-Cad, human VE-cadherin.

weak expression of the human-specific CD31 (hCD31) gene, but not of hVE-Cad, another EC marker, whereas GM-PB MNCs revealed very weak expression of the hCD31 gene but no expression, for the most part, of hCD34 or hVE-Cad (Fig. 1E). These results indicate that human GM-PB CD34+ cells contain a large EPC/hematopoietic stem cell (HSC) population compared with GM-PB MNCs.

Human GM-PB CD34+ Cell-Derived Vasculogenesis

To histologically prove the existence of surviving human cells and the phenomenon of human cell-derived vasculogenesis, immunohistochemical staining for HNA, HLA-ABC, and UEA-1, a human-specific EC marker, was performed using tissue samples obtained 1 week after cell administration. Abundant human cells were detected as HNA+/DAPI+ cells at the peri-injury site in animals treated with CD34+ cells, whereas no human cells were identified in the control group (Fig. 2A). Differentiated human ECs derived from the transplanted CD34+ cells or MNCs were detected as UEA-1+/HLA-ABC+ cells in the vasculature in the peri-injury area, whereas UEA-1+/HLA-ABC+ cells were not identified in the control group (Fig. 2B). The number of UEA-1+/HLA-ABC+ cells was significantly higher in the CD34+ group compared with the MNC group (hCD34+, 119.5 ± 20.0; hMNC, 54.0 ± 16.5; control, 0.0 ± 0.0 per mm^2; $p < .01$ for hCD34+ vs. control; $p <$

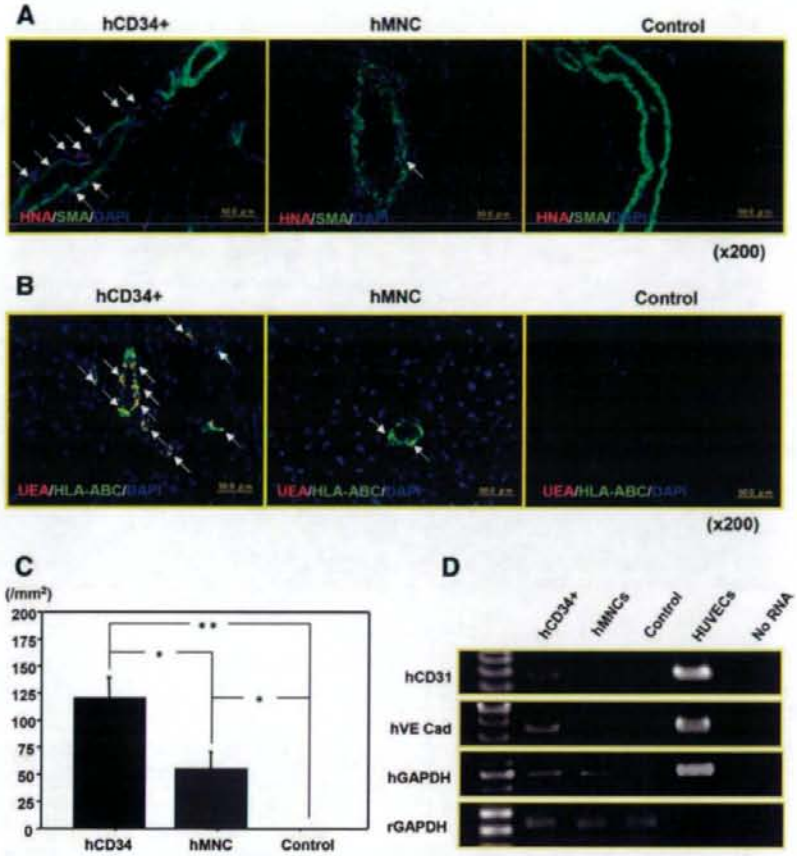

Figure 2. Human granulocyte-stimulating factor-mobilized peripheral blood CD34+ cell-derived vasculogenesis. **(A):** Immunohistochemistry of tissue sample at week 1 demonstrated that numerous human cells, identified by the red fluorescence of HNA (arrows), were detected at the peri-injury site in the hCD34+ group, whereas few human cells were detected in the hMNC group, and no human cells were identified in the control group. Arterioles and nuclei are depicted by the green fluorescence of SMA and by the blue fluorescence of DAPI staining, respectively (magnification, ×200). **(B):** Differentiated human endothelial cells (ECs) derived from the transplanted CD34+ cells or MNCs were detected as UEA-1+/HLA-ABC+ cells (arrows) in the vasculature in the peri-injury area, whereas UEA-1+ cells were not identified in the control group (magnification, ×200). **(C):** The numbers of UEA-1+/HLA-ABC+ cells were significantly higher in the CD34+ group compared with the MNC group and the control group. *, $p < .05$; **, $p < .01$. **(D):** Representative reverse transcription-polymerase chain reaction analysis performed on tissue sample collected 1 week after surgery. The gene expression of human-specific EC markers (hCD31 and hVE-Cad) was detected in the hCD34+ group but not in the hMNC group or control group. Simply cultured HUVECs were used for positive control for human endothelial genes. Abbreviations: DAPI, 4,6-diamidino-2-phenylindole; hCD31, human CD31; hCD34, human CD34; hGAPDH, human glyceraldehyde-3-phosphate dehydrogenase; HLA-ABC, human leukocyte antigen-ABC; hMNC, human mononuclear cell; HNA, human nuclei antibody; HUVEC, human umbilical vein endothelial cell; hVE Cad, human VE-cadherin; rGAPDH, rat glyceraldehyde-3-phosphate dehydrogenase; SMA, smooth muscle actin; UEA, *Ulex europaeus* lectin.

.05 for hCD34+ vs. hMNC and hMNC vs. control) (Fig. 2C). To further confirm this phenomenon in terms of transcription, RT-PCR analysis of tissue RNA isolated from the peri-injury site was performed. The molecular approach revealed the gene expression of human-specific EC markers (hCD31 and hVE-Cad) in the CD34+ group, but not in the other groups (Fig. 2D). These results indicate that human GM-PB CD34+ cells efficiently differentiate into ECs in a ligament injury-induced environment.

Enhancement of Intrinsic Angiogenesis in Animals Receiving CD34+ Cells

Enhanced angiogenesis by recipient cells following cell transplantation was further confirmed by immunostaining for rat-specific markers. Vascular staining with isolectin B4 (marker for rat ECs but not human ECs) using tissue samples at week 2 postinjury demonstrated enhanced neovascularization around the granulation area (Fig. 3A, zone a) in the CD34+ group compared with the other groups (Fig. 3C). Neovascularization assessed by capillary density was significantly enhanced in the CD34+ group compared with both the MNC group and the control group (hCD34+, 301.0 ± 18.1; hMNC, 209.5 ± 32.3; control, 108.6 ± 15.6 [number of capillary profiles per mm^2]; $p < .01$ for hCD34+ vs. control; $p < .05$ for hCD34+ vs. hMNC and hMNC vs. control) (Fig. 3D).

Furthermore, we performed quantitative real-time RT-PCR experiments to investigate rat VEGF mRNA expression around the MCL injury sites. Gene expression of rVEGF at

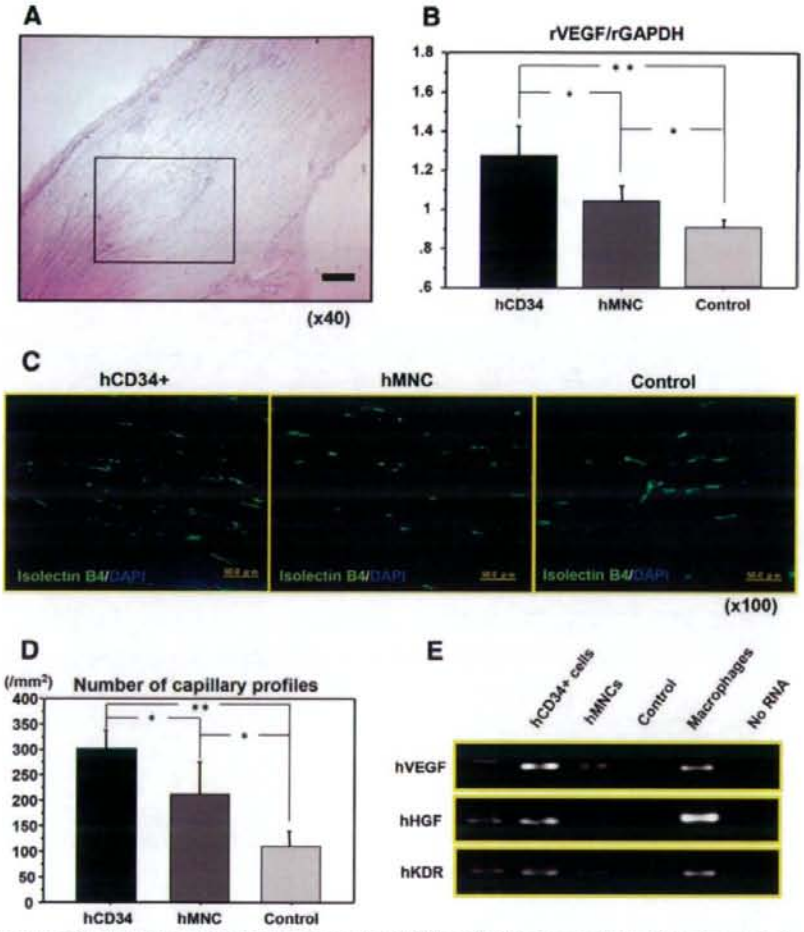

Figure 3. Enhancement of intrinsic angiogenesis in animals receiving CD34+ cells. **(A):** Representative photomicrograph of a hematoxylin and eosin-stained sample. The black box indicates a granulation area. Scale bars = 200 μm (magnification, ×40). **(B):** Real-time reverse transcription (RT)-polymerase chain reaction (PCR) using tissue sample at week 1 demonstrated that rVEGF was significantly higher in the hCD34+ group compared with the hMNC group and the control group. *, $p < .05$; **, $p < .01$. **(C):** Staining of tissue samples collected 2 weeks after injury with the rat-specific endothelial marker isolectin B4 (green fluorescence) demonstrated enhanced neovascularization around the granulation area of the hCD34+ group with respect to the hMNC group and the control group (magnification, ×200). **(D):** Neovascularization assessed by capillary density was significantly enhanced in the hCD34+ group compared with the hMNC group and the control group. *, $p < .05$; **, $p < .01$. **(E):** Reverse transcription-polymerase chain reaction analysis of tissue sample at 1 week demonstrated that the gene expression of human-specific angiogenic factors (hVEGF, hHGF) were higher in the hCD34+ group compared with the hMNC group and the control group. Simply cultured macrophages were used for positive control for human endothelial genes. Abbreviations: DAPI, 4,6-diamidino-2-phenylindole; hCD34, human CD34; hHGF, human hepatocyte growth factor; hKDR, human kinase insert domain-containing receptor; hMNC, human mononuclear cell; hVEGF, human vascular endothelial growth factor; rGAPDH, rat glyceraldehyde-3-phosphate dehydrogenase; rVEGF, rat vascular endothelial growth factor.

week 1 was significantly higher in animals receiving GM-PB CD34+ cells compared with both the MNC group and the control group (hCD34+, 1.269 ± 0.078; hMNC,1.036 ± 0.041; control, 0.901 ± 0.018 relative to rGAPDH; $p < .01$ for hCD34 vs. control; $p < .05$ for hCD34 vs. hMNC and hMNC vs. control) (Fig. 3B).

To evaluate whether transplanted CD34+ cells contribute intrinsic vascularization in terms of the paracrine effect compared with MNCs, we confirmed that transplanted CD34+ cells released a greater amount of angiogenic factors (hVEGF, hKDR, and hHGF) than MNCs at the peri-injury site (Fig. 3E). These results indicate that administration of human GM-PB CD34+ cells may enhance intrinsic angiogenesis in an autocrine/paracrine manner.

Human GM-PB CD34+ Cell-Derived Differentiation into Hematopoietic/Inflammatory Cells

To identify human hematopoietic/inflammatory cells in the rat injury site of MCL, immunohistochemistry was performed with a human-specific antibody against CD45, known to be a hematopoietic/inflammatory cell marker. Differentiated human CD45+ hematopoietic/inflammatory cells derived from the transplanted CD34+ cells in the peri-injury area were detected at a lower level than those from the MNCs (Fig. 4A). The

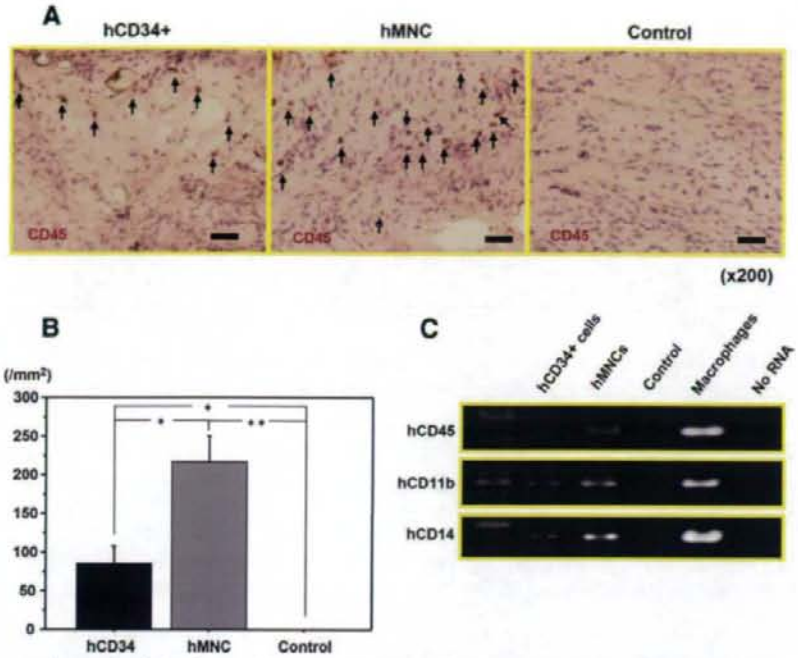

Figure 4. Human granulocyte-stimulating factor-mobilized peripheral blood CD34+ cell-derived differentiation into hematopoietic/inflammatory cells. **(A):** Staining of tissue samples at week 1 with the human-specific antibody against CD45 (arrows) demonstrated that fewer CD45+ cells in the peri-injury area were detected in the hCD34+ group compared with the hMNC group, whereas no CD45+ cells were detected in the control group. Scale bars = 50 μm. **(B):** The number of CD45+ cells at the peri-injury site was significantly lower in the hCD34+ group compared with the hMNC group. *, $p < .05$; **, $p < .01$. **(C):** Reverse transcription-polymerase chain reaction analysis using tissue samples at week 1 demonstrated that the gene expression of human-specific hematopoietic/inflammatory cell markers (hCD45, hCD11b, and hCD14) was detected at higher levels in the hMNC group compared with the hCD34+ group, whereas no gene expressions were identified in the control group. Simply cultured macrophages were used for positive control. Abbreviations: hCD11b, human CD11b; hCD14, human CD14; hCD34, human CD34; hCD45, human CD45; hMNC, human mononuclear cell.

number of CD45+ cells was significantly lower in the CD34+ group compared with the MNC group (hCD34+, 84.5 ± 24.1; hMNC, 216.0 ± 34.2; control, 0.0 ± 0.0 per mm^2; $p < .01$ for hMNC vs. control; $p < .05$ for hCD34+ vs. hMNC and hCD34 vs. control) (Fig. 4B).

To further evaluate differentiation into hematopoietic/inflammatory cells in terms of transcription, RT-PCR analysis of tissue RNA isolated from the injury site was performed. The results revealed that the gene expression of human-specific hematopoietic/inflammatory cell markers (hCD45, hCD11b, and hCD14) was strong in the MNC group compared with the CD34+ group, while no expression in the control group (Fig. 4C). These results indicate that human GM-PB CD34+ cell-derived differentiation into hematopoietic/inflammatory cells was lower than MNCs-derived differentiation.

Molecular, Morphological, and Functional Recovery of Ligament Injury in Animals Receiving CD34+ Cell Transplantation

Ligament healing in each group was assessed by real-time RT-PCR of rTeM and rCol1A2, which are ligament-related markers [34–36]. Gene expression of rTeM at week 1 was significantly higher in animals receiving GM-PB CD34+ cells compared with both the MNC group and the control group (hCD34+, 1.394 ± 0.075; hMNC, 0.989 ± 0.013; control, 0.948 ± 0.022; $p < .05$ for hCD34+ vs. control and hCD34+ vs. hMNC) (Fig. 5C). Gene expression of rCol1A2 at week 1 was significantly higher in animals receiving GM-PB CD34+ cells compared with the other groups (hCD34+, 1.447 ± 0.094; hMNC, 1.062 ± 0.064; control, 0.978 ± 0.067 per mm^2; $p < .01$ for hCD34 vs. control; $p < .05$ for hCD34 vs. hMNC).

Morphological recovery of ligament injury in each group was evaluated by macroscopic and histological examinations. Macroscopic inspection demonstrated that the ligament significantly healed in 33% of rats (two of six) at week 2 and in all rats at week 4 (six of six) in the CD34+ group compared with 16% of rats (one of six) at week 2 and 33% of rats (two of six) at week 4 in the MNC groups, and 0% of rats (zero of six) at week 2 and 33% of rats (two of six) in the control groups (Fig. 5A). Histological evaluation with HE staining demonstrated almost complete healing as a fibrous continuity at week 2 and complete healing, except for a small number of inflammatory cells, at week 4 in the CD34+ group (Fig. 5B). In contrast, the laceration site could easily be observed in spite of the existence of higher cellularity of inflammatory cells at week 2, and the healing process had not yet been completed by week 4 in the other groups (Fig. 5B).

Functional recovery of ligament injury in each group was evaluated by failure load of biochemical tensile test. Failure load obtained at week 2 was significantly higher in the CD34+ group compared with both the MNC and the control groups (sham-exposed group, 8,608.203 ± 636.247; hCD34+, 6,734.766 ± 618.357; hMNC, 3,530.606 ± 1,385.589; control, 3,823.325 ± 95.538 mN; $p < .05$ for hCD34 vs. hMNC and hCD34 vs.

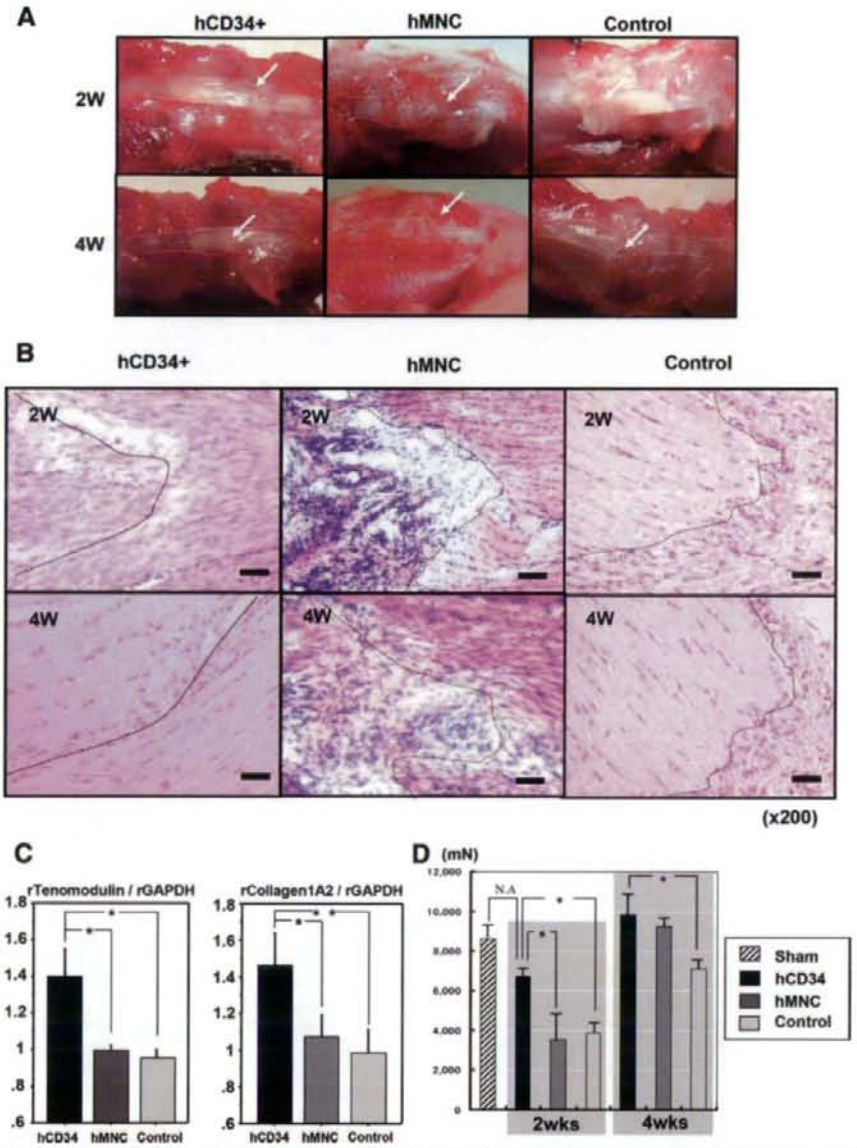

Figure 5. Molecular, morphological, and biomechanical recovery of ligament injury in animals receiving hCD34+ cell transplantation. **(A):** Representative macroscope of the peri-injury site of medial collateral ligament (MCL) (arrows). The ligament significantly healed in 33% of rats (two of six) at W 2 and all rats at W 4 (six of six) in the hCD34+ group compared with 16% of rats (one of six) at W 2 and 33% of rats (two of six) at W 4 in the hMNC group, and 0% of rats (zero of six) at W 2 and 33% of rats (two of six) at W 4 in the control group. White dot lines indicate MCL. **(B):** Representative histological evaluation performed on hematoxylin and eosin-stained samples. Treated animals (hCD34+ group) presented almost complete healing as a fibrous continuity at W 2 and complete healing at W 4, except that a few inflammatory cells were found. In contrast, the laceration site could easily be observed in spite of the existence of higher cellularity of inflammatory cells at W 2, and the healing process was not yet completed by W 4 in the hMNC group or the control group (magnification, ×200). Black dot lines indicate edge of the injured MCL. Scale bars = 50 μm. **(C):** Real-time reverse transcription-polymerase chain reaction using tissue sample at W 1 demonstrated that the gene expression of rTenomodulin and rCollagen1A2 was significantly higher in the hCD34+ group compared with the MNC group and control group. *, $p < .05$; **, $p < .01$. **(D):** Failure load of tensile test demonstrated that biomechanical strength was significantly higher in the hCD34+ group compared with both the hMNC and the control groups at W 2. At W 4, failure load obtained in the hCD34+ group, not the hMNC group, was significantly higher compared with the control group. *, $p < .05$. Abbreviations: hCD34, human CD34; hMNC, human mononuclear cell; rCollagen1A2, rat collagen1A2; rGAPDH, rat glyceraldehyde-3-phosphate dehydrogenase; rTenomodulin, rat tenomodulin; W, weeks; wks, weeks.

control) (Fig. 5D). At week 4, the failure load obtained in the CD34+ group, but not that obtained in the MNC group, was significantly higher compared with the control group (CD34+, 9,843.817 ± 1,216.443; hMNC, 9,241.084 ± 467.519; control, 7,085.041 ± 472.701 mN; $p < .05$ for hCD34 vs. control) (Fig. 5D). These results indicate that the MCL injuries in the immunodeficient rats were not only molecularly and morphologically healed but also biomechanically healed by the administration of human GM-PB CD34+ cells.

Inhibition of Intrinsic Angiogenesis by Antiangiogenic Agent in Animals Receiving CD34+ Cells

To investigate the hypothesis that neovascularization is essential to support endogenous ligament healing, an antiangiogenic agent, sFlit1, which is known to inhibit proliferation of endothelial cells, was injected for 14 days. Vascular staining with isolectin B4 (marker for rat ECs but not human ECs) using tissue samples at week 2 postinjury demonstrated inhibited neovascularization around the peri-injury site in the sFlt1 group compared with the PBS group (Fig. 6A). Neovascularization, assessed by capillary density, was significantly inhibited in the sFlt group compared with the PBS group (sFlt1, 221.7 ± 21.191; PBS, 303.2 ± 20.299 per mm^2; $p < .05$) (Fig. 6B). Macroscopic inspection demonstrated that the ligament was significantly healed in 33% of rats (two of six) at week 2 and in all rats (six of six) at week 4 in the PBS group compared with 0% of rats (zero of six) at week 2 and 33% of rats (two of six) at week 4 in the sFlt1 groups (Fig. 6C). Histological evaluation with HE staining demonstrated a fibrous continuity at week 2 and almost complete healing, except for a small number of inflammatory cells, at week 4 in PBS group (Fig. 6D). In contrast, the laceration site could easily be observed in spite of the existence of inflammatory cells at week 2, and the healing process had not yet been completed at week 4 in the sFlt1 group (Fig. 6D). These results indicate that neovascularization is essential to support endogenous ligament healing.

Discussion

Rapid revascularization of injured, ischemic, and regenerating organs is essential to restore organ function. The angiogenic switch initiates the revascularization process and involves recruitment of EPCs that assemble into neovessels [37–43]. In the category of ligament regeneration, much effort has been focused on delivering angiogenic factors to accelerate tissue revascularization [6, 7, 9, 10, 44]. In such cytokines, VEGF has been recognized as the most potent angiogenic factor. Although VEGF has also been reported to promote angiogenesis in ligament healing, it does not seem to affect the mechanical properties [45]. Therefore, a new strategy needs to be developed to accelerate the remodeling of ligament injury. With such recognition, transplantation of EPCs as a cell-based therapy might offer another potential strategy to engineer ligament healing via angiogenesis and vasculogenesis. Recently, EPC investigation for promoting tissue neovascularization has widened those applications to various categories of regenerative medicine. In the immunodeficient rat model of acute myocardial infarction, transplanted human CD34+ cells or ex vivo-expanded EPCs incorporate into the site of the myocardial neovascularization, differentiate into mature ECs, augment capillary density, inhibit myocardial fibrosis and apoptosis, and preserve the left ventricular function [22–24]. Systemic administration of human cord blood-derived CD34+ cells to immunocompromised mice subjected to stroke 48 hours earlier induces neovascularization in the ischemic zone and provides a favorable environment for neuronal regeneration [27]. Transplantation of peripheral blood CD34+ cells to promote revascularization could improve wound healing in full-thickness skin wounds of diabetic mice [26]. Similarly, we quite recently reported that human peripheral blood CD34+ cells, systemically transplanted into an immunodeficient rat model of nonhealing fracture, were recruited to the fracture site, developed a favorable environment for fracture healing by enhancing vasculogenesis and angiogenesis, and finally led to functional recovery from fracture [30].

We used a reproducible animal model of MCL injury, clearly relevant to the clinical situation of ligament injury. The atelocollagen gel that we used in this study with CD34+ cells has already been confirmed not to disturb cell viability during cartilage and bone regeneration [32, 46, 47]. In the present study, we proved that CD34+ cells survived by double immunohistochemistry of human nuclei antigen and DAPI. We also identified in vivo differentiation of human peripheral blood CD34+ cells into ECs not only by immunohistochemistry but by RT-PCR for human-specific cell markers. Although this differentiation has been confirmed in the various animal models of diseases, such as limb ischemia, myocardial infarction, stroke, and diabetic wound, evidence of vasculogenesis for ligament healing has not previously been reported. In the present study, the CD34+ population that we used was 99% positive for CD45 by FACS analysis. Recently, it has been reported that CD34+/CD45− cells, not CD34+/CD45+ cells, formed ECs [48]. However, in the present study, we confirmed lower differentiation of CD34+ cells (99% positive for CD45) into CD45+ hematopoietic/inflammatory cells compared with MNCs (91% positive for CD45) by immunohistochemistry and RT-PCR for human-specific cell markers in the perifracture site. These results suggest that there is a difference in maturation between CD34+ cells and MNCs during the healing process. These findings, consistent with the previous study in a rat myocardial ischemic model [49], also suggest that hemorrhage/inflammation in the acute phase may be harmful for survival and differentiation of the transplanted cells in the chronic phase. These results indicate that purified CD34+ cell transplantation may have more potential for ligament healing compared with total MNC transfer.

In addition to these sensitive assessments of donor cell differentiation at the incorporated site, quantitative histochemical analysis for rat ECs revealed the enhancement of intrinsic angiogenesis by recipient cells following the administration of human CD34+ cells. Recipient VEGF expression by real-time RT-PCR was also proven to be enhanced by human CD34+ cell transplantation. In addition to this endogenous effect, human CD34+ cells were reported to secrete numerous angiogenic factors, including VEGF, hepatocyte growth factor, fibroblast growth factor 2 (FGF2), and IGF1 in vitro [50, 51]. The present study also demonstrated gene expression of human angiogenic factors, including VEGF and HGF, by human CD34+ cell transplantation at the peri-injury site. In addition, we proved that the inhibition of angiogenesis by soluble Flt1 suppressed not only angiogenesis/vasculogenesis but also intrinsic ligament healing, indicating that angiogenic factors released by the transplanted CD34+ cells contribute, at least in part, to ligament healing in paracrine manner, as we reported previously [30].

On the other hand, some researchers recently reported that CD34+ cells have a potency to differentiate into not only ECs but also mural perivascular cells (i.e., pericytes and smooth muscle cells) [20, 52]. Similarly, it has been reported recently that vascular pericytes may arise from CD34+ cells [53]. Although we did not address direct evidence of the differentiation capacity of CD34+ cells toward mural vascular cells, our RT-PCR analysis of whole peri-injury tissues may indicate that the

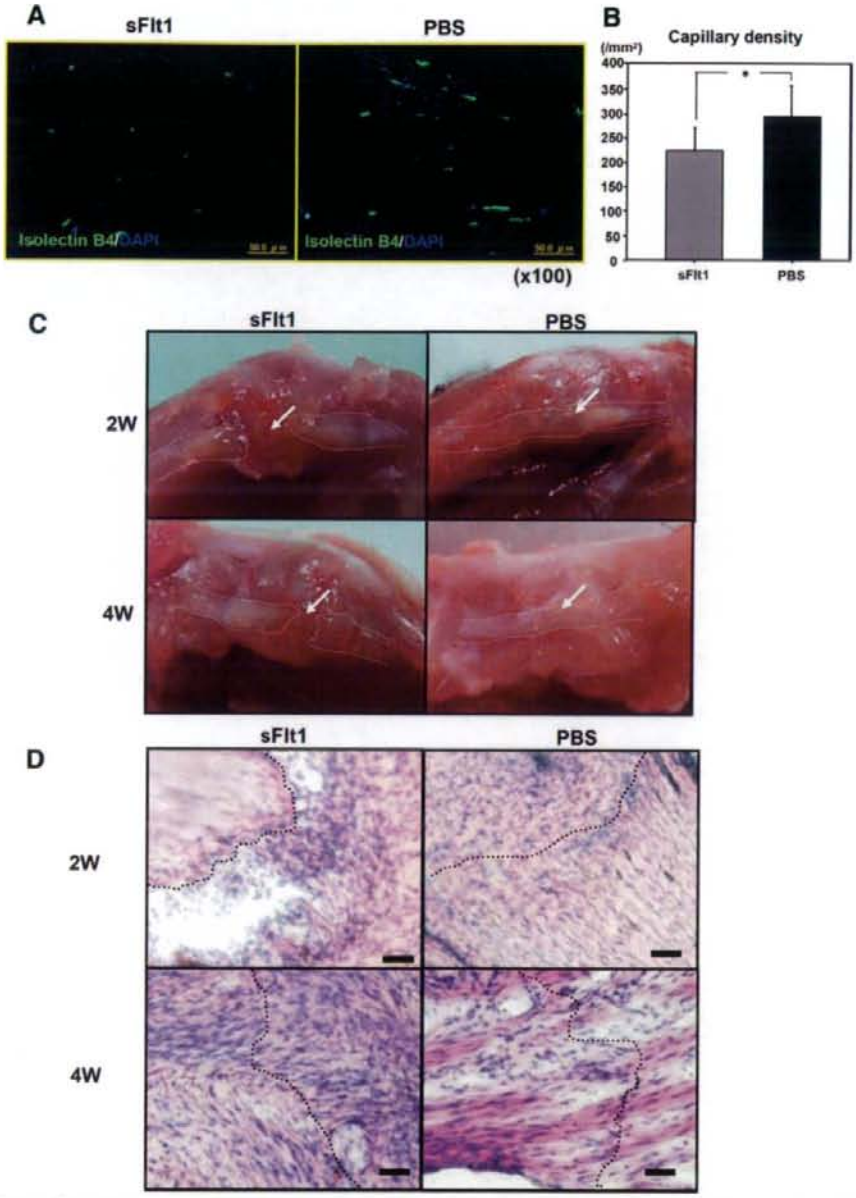

Figure 6. Inhibition of intrinsic angiogenesis by antiangiogenic agent in animals receiving CD34+ cells. **(A):** Staining of tissue samples collected 2 W after injury with the rat-specific endothelial marker isolectin B4 (green fluorescence) demonstrated inhibited neovascularization around the peri-injury site in the sFlt1 group compared with the phosphate-buffered saline (PBS) group. **(B):** Number of capillary profiles demonstrated that neovascularization was significantly inhibited in the sFlt1 group compared with the PBS group. *, $p < .05$. **(C):** Representative macroscope of the peri-injury site of medial collateral ligament (MCL) (arrows). The ligament healing was significantly inhibited in 0% of rats (zero of six) at W 2 and 33% of rats (two of six) at W 4 in the sFlt1 group compared with 33% of rats (two of six) at W 2 and all rat (six of six) at W 4 in the PBS group. White dot lines indicate MCL. **(D):** Representative histological evaluation performed on hematoxylin and eosin-stained samples. Angiogenesis-inhibited animals (sFlt1 group) presented the laceration observed at W 2 and the existence of higher cellularity of inflammatory cells detected at W 4, whereas in the PBS group, a fibrous continuity was already identified at W 2, and injured ligament was almost completely healed at W 4. Dotted lines indicate edges of the injured MCL. Scale bars = 50 μm. Abbreviations: DAPI, 4,6-diamidino-2-phenylindole; PBS, phosphate-buffered saline; sFlt1, soluble Flt1; W, week(s).

possibility remains. These findings suggest that CD34+ cells may be involved and pooled as vascular progenitor cells in the vascular wall. In addition, EPCs have been also reported to be mobilized and vascularized via an autocrine loop that involves

FGF2 [51, 54]. Considering these reports, the present study suggests that microenvironmental interaction between vasculogenesis and ligament healing may involve not only autocrine/paracrine regulatory factors but also direct cellular communications in developing CD34+ cells.

The environmental contribution of CD34+ cells resulted in morphological and biomechanical healing of the ligament. Macroscopic inspection and histological HE staining demonstrated enhancement of ligament healing and remodeling after CD34+ cell transplantation. Real-time RT-PCR analysis using a tissue sample at the peri-injury site also demonstrated enhancement of collagen1A2 (Col1A2) and tenomodulin (TeM) gene expression by CD34+ cell transplantation. Col1A2 and TeM were reported to be markers for tenocytes [34–36]. Expression of TeM was reported to be tightly associated with dense connective tissue, such as ligament and tendon, and to be a marker for mature tenocytes [36]. Tensile test also demonstrated enhancement of the biomechanical strength of ligament by CD34+ cell transplantation. These findings strongly suggest that peripheral blood CD34+ cells have significant potential for therapeutic application to the damaged ligament.

BM nuclear cells were also reported to serve as a vehicle for therapeutic molecules, as well as a source for enhancing healing of ligaments [31]. It remains to be clarified whether circulating CD34+ cell transplantation is superior to BM cell therapy in terms of efficacy and safety for ligament healing; however, cell harvest from peripheral blood does provide benefits in that (a) it is less invasive and safer than BM aspiration under general anesthesia, and (b) magnetic sorting of CD34+ cells has been clinically applied in the hematology field for many years [55, 56].

Although we believe that our findings provide novel evidence that circulating CD34+ cells have significant potential for therapeutic application to the damaged ligament, our present study has some limitations. The GM-PB CD34+ cells used in this study require the use of mobilizing growth factor in a clinical setting, not nonmobilized CD34+ cells. Although we have to consider the side effects in using mobilizing growth factor even if they are minimal, the benefit of the use of mobilizing growth factor is the large cell number. Ideally, we should expand nonmobilized CD34+ cells to a high enough number to be efficiently transplanted. On the other hand, we have already clarified the multidifferentiation capacity of CD34+ cells into osteoblasts and ECs in the previous bone fracture model [30]. Although CD34+ cells may have a potency to differentiate into fibroblasts or fibrochondrocytes, we could not demonstrate a direct contribution of CD34+ cells to ligament healing. We also need to test the effectiveness of this treatment in a large-animal model, such as a canine anterior cruciate ligament reconstruction model, so as to confirm the clinical feasibility.

In conclusion, human circulating CD34+ cells have a potent vasculogenesis mechanism in the MCL injury-induced environment, enabling them to make a remarkable contribution to morphological ligament healing. The technical feasibility in a clinical situation and the present preclinical findings demonstrating morphological ligament healing through concurrent vasculogenesis strongly suggest promising results for the future clinical application of circulating CD34+ cells for ligament healing and remodeling.

ACKNOWLEDGMENTS

We thank Janina Tubby for editing assistance in preparing the manuscript. K.T. and T.M. contributed equally to this work.

DISCLOSURE OF POTENTIAL CONFLICTS OF INTEREST

The authors indicate no potential conflicts of interest.

REFERENCES

1 Weiss JA, Woo SL, Ohland KJ et al. Evaluation of a new injury model to study medial collateral ligament healing: Primary repair versus nonoperative treatment. J Orthop Res 1991;9:516–528.
2 Woo SL, Inoue M, McGurk-Burleson E et al. Treatment of the medial collateral ligament injury. II: Structure and function of canine knees in response to differing treatment regimens. Am J Sports Med 1987; 15:22–29.
3 Day CS, Kasemkijwattana C, Menetrey J et al. Myoblast-mediated gene transfer to the joint. J Orthop Res 1997;15:894–903.
4 Hildebrand KA, Deie M, Allen CR et al. Early expression of marker genes in the rabbit medial collateral and anterior cruciate ligaments: The use of different viral vectors and the effects of injury. J Orthop Res 1999;17:37–42.
5 Andriacchi T, Sabiston P, DeHaven K, et al. Ligament: Injury and repair. In: Woo SL-Y, Buckwalter JA eds. Injury and Repair of the Musculoskeletal Soft Tissues. Chicago, IL: American Academy of Orthopaedic Surgeons. 1988:103–128.
6 Hildebrand KA, Woo SL, Smith DW et al. The effects of platelet-derived growth factor-BB on healing of the rabbit medial collateral ligament. An in vivo study. Am J Sports Med 1998;26:549–554.
7 Batten ML, Hansen JC, Dahners LE. Influence of dosage and timing of application of platelet-derived growth factor on early healing of the rat medial collateral ligament. J Orthop Res 1996;14:736–741.
8 Kuroda R, Kurosaka M, Yoshiya S et al. Localization of growth factors in the reconstructed anterior cruciate ligament: Immunohistological study in dogs. Knee Surg Sports Traumatol Arthrosc 2000;8:120–126.
9 Letson AK, Dahners LE. The effect of combinations of growth factors on ligament healing. Clin Orthop Relat Res 1994;(308):207–212.
10 Nakamura N, Shino K, Natsuume T et al. Early biological effect of in vivo gene transfer of platelet-derived growth factor (PDGF)-B into healing patellar ligament. Gene Ther 1998;5:1165–1170.
11 Woo SL, Abramowitch SD, Kilger R et al. Biomechanics of knee ligaments: Injury, healing, and repair. J Biomech 2006;39:1–20.
12 Frank C, Bray R, Hart D. Soft tissue healing. In: Fu F, Harner CD, Vince KG, eds. Knee Surgery. Baltimore: Williams and Wilkins: 1994:189–229.
13 Woo SL, Hildebrand K, Watanabe N et al. Tissue engineering of ligament and tendon healing. Clin Orthop Relat Res 1999;(367 suppl): S312–S323.
14 Pardanaud L, Yassine F, Dieterlen-Lievre F. Relationship between vasculogenesis, angiogenesis and haemopoiesis during avian ontogeny. Development 1989;105:473–485.
15 Asahara T, Masuda H, Takahashi T et al. Bone marrow origin of endothelial progenitor cells responsible for postnatal vasculogenesis in physiological and pathological neovascularization. Circ Res 1999;85: 221–228.
16 Asahara T, Murohara T, Sullivan A et al. Isolation of putative progenitor endothelial cells for angiogenesis. Science 1997;275:964–967.
17 Risau W, Sariola H, Zerwes HG et al. Vasculogenesis and angiogenesis in embryonic-stem-cell-derived embryoid bodies. Development 1988; 102:471–478.
18 Assmus B, Schachinger V, Teupe C et al. Transplantation of Progenitor Cells and Regeneration Enhancement in Acute Myocardial Infarction (TOPCARE-AMI). Circulation 2002;106:3009–3017.
19 Britten MB, Abolmaali ND, Assmus B et al. Infarct remodeling after intracoronary progenitor cell treatment in patients with acute myocardial infarction (TOPCARE-AMI): Mechanistic insights from serial contrast-enhanced magnetic resonance imaging. Circulation 2003;108: 2212–2218.
20 Iwasaki H, Kawamoto A, Ishikawa M et al. Dose-dependent contribution of CD34-positive cell transplantation to concurrent vasculogenesis and cardiomyogenesis for functional regenerative recovery after myocardial infarction. Circulation 2006;113:1311–1325.
21 Kalka C, Masuda H, Takahashi T et al. Transplantation of ex vivo expanded endothelial progenitor cells for therapeutic neovascularization. Proc Natl Acad Sci U S A 2000;97:3422–3427.

22 Kawamoto A, Gwon HC, Iwaguro H et al. Therapeutic potential of ex vivo expanded endothelial progenitor cells for myocardial ischemia. Circulation 2001;103:634–637.
23 Kawamoto A, Tkebuchava T, Yamaguchi J et al. Intramyocardial transplantation of autologous endothelial progenitor cells for therapeutic neovascularization of myocardial ischemia. Circulation 2003; 107:461–468.
24 Kocher AA, Schuster MD, Szabolcs MJ et al. Neovascularization of ischemic myocardium by human bone-marrow-derived angioblasts prevents cardiomyocyte apoptosis, reduces remodeling and improves cardiac function. Nat Med 2001;7:430–436.
25 Murohara T, Ikeda H, Duan J et al. Transplanted cord blood-derived endothelial precursor cells augment postnatal neovascularization. J Clin Invest 2000;105:1527–1536.
26 Sivan-Loukianova E, Awad OA, Stepanovic V et al. CD34+ blood cells accelerate vascularization and healing of diabetic mouse skin wounds. J Vasc Res 2003;40:368–377.
27 Taguchi A, Soma T, Tanaka H et al. Administration of CD34+ cells after stroke enhances neurogenesis via angiogenesis in a mouse model. J Clin Invest 2004;114:330–338.
28 Takahashi T, Kalka C, Masuda H et al. Ischemia- and cytokine-induced mobilization of bone marrow-derived endothelial progenitor cells for neovascularization. Nat Med 1999;5:434–438.
29 Werner N, Junk S, Laufs U et al. Intravenous transfusion of endothelial progenitor cells reduces neointima formation after vascular injury. Circ Res 2003;93:e17–e24.
30 Matsumoto T, Kawamoto A, Kuroda R et al. Therapeutic potential of vasculogenesis and osteogenesis promoted by peripheral blood CD34-positive cells for functional bone healing. Am J Pathol 2006;169: 1440–1457.
31 Watanabe N, Woo SL, Papageorgiou C et al. Fate of donor bone marrow cells in medial collateral ligament after simulated autologous transplantation. Microsc Res Tech 2002;58:39–44.
32 Hisatome T, Yasunaga Y, Yanada S et al. Neovascularization and bone regeneration by implantation of autologous bone marrow mononuclear cells. Biomaterials 2005;26:4550–4556.
33 Ito Y, Ochi M, Adachi N et al. Repair of osteochondral defect with tissue-engineered chondral plug in a rabbit model. Arthroscopy 2005;21: 1155–1163.
34 Docheva D, Hunziker EB, Fassler R et al. Tenomodulin is necessary for tenocyte proliferation and tendon maturation. Mol Cell Biol 2005;25: 699–705.
35 Shukunami C, Oshima Y, Hiraki Y. Chondromodulin-I and tenomodulin: A new class of tissue-specific angiogenesis inhibitors found in hypovascular connective tissues. Biochem Biophys Res Commun 2005;333:299–307.
36 Shukunami C, Takimoto A, Oro M et al. Scleraxis positively regulates the expression of tenomodulin, a differentiation marker of tenocytes. Dev Biol 2006;298:234–247.
37 Carmeliet P, Jain RK. Angiogenesis in cancer and other diseases. Nature 2000;407:249–257.
38 Folkman J. Angiogenesis in cancer, vascular, rheumatoid and other disease. Nat Med 1995;1:27–31.
39 Folkman J. Therapeutic angiogenesis in ischemic limbs. Circulation 1998;97:1108–1110.
40 Hanahan D, Folkman J. Patterns and emerging mechanisms of the angiogenic switch during tumorigenesis. Cell 1996;86:353–364.
41 Pepper MS. Manipulating angiogenesis. From basic science to the bedside. Arterioscl Thromb Vasc Biol 1997;17:605–619.
42 Risau W. Mechanisms of angiogenesis. Nature 1997;386:671–674.
43 Yancopoulos GD, Davis S, Gale NW et al. Vascular-specific growth factors and blood vessel formation. Nature 2000;407:242–248.
44 Nakamura N, Timmermann SA, Hart DA et al. A comparison of in vivo gene delivery methods for antisense therapy in ligament healing. Gene Ther 1998;5:1455–1461.
45 Ju YJ, Tohyama H, Kondo E et al. Effects of local administration of vascular endothelial growth factor on properties of the in situ frozen-thawed anterior cruciate ligament in rabbits. Am J Sports Med 2006;34: 84–91.
46 Murakami T, Fujimoto Y, Yasunaga Y et al. Transplanted neuronal progenitor cells in a peripheral nerve gap promote nerve repair. Brain Res 2003;974:17–24.
47 Zhang X, Mitsuru A, Igura K et al. Mesenchymal progenitor cells derived from chorionic villi of human placenta for cartilage tissue engineering. Biochem Biophys Res Commun 2006;340:944–952.
48 Case J, Mead LE, Bessler WK et al. Human CD34+AC133+VEGFR-2+ cells are not endothelial progenitor cells but distinct, primitive hematopoietic progenitors. Exp Hematol 2007;35:1109–1118.
49 Kawamoto A, Iwasaki H, Kusano K et al. CD34-positive cells exhibit increased potency and safety for therapeutic neovascularization after myocardial infarction compared with total mononuclear cells. Circulation 2006;114:2163–2169.
50 Janowska-Wieczorek A, Majka M, Ratajczak J et al. Autocrine/paracrine mechanisms in human hematopoiesis. STEM CELLS 2001;19:99–107.
51 Majka M, Janowska-Wieczorek A, Ratajczak J et al. Numerous growth factors, cytokines, and chemokines are secreted by human CD34(+) cells, myeloblasts, erythroblasts, and megakaryoblasts and regulate normal hematopoiesis in an autocrine/paracrine manner. Blood 2001;97: 3075–3085.
52 Yeh ET, Zhang S, Wu HD et al. Transdifferentiation of human peripheral blood CD34+-enriched cell population into cardiomyocytes, endothelial cells, and smooth muscle cells in vivo. Circulation 2003;108:2070–2073.
53 Howson KM, Aplin AC, Gelati M et al. The postnatal rat aorta contains pericyte progenitor cells that form spheroidal colonies in suspension culture. Am J Physiol Cell Physiol 2005;289:C1396–C1407.
54 Fontaine V, Filipe C, Werner N et al. Essential role of bone marrow fibroblast growth factor-2 in the effect of estradiol on reendothelialization and endothelial progenitor cell mobilization. Am J Pathol 2006;169: 1855–1862.
55 Kanz L, Brugger W. Retraction: Reconstitution of hematopoiesis after high-dose chemotherapy by autologous progenitor cells generated ex vivo. N Engl J Med 2001;345:64.
56 Kessinger A, Armitage JO. The evolving role of autologous peripheral stem cell transplantation following high-dose therapy for malignancies. Blood 1991;77:211–213.

Journal of Cellular Physiology

Fracture Induced Mobilization and Incorporation of Bone Marrow-Derived Endothelial Progenitor Cells for Bone Healing

TOMOYUKI MATSUMOTO,[1,2] YUTAKA MIFUNE,[1,2] ATSUHIKO KAWAMOTO,[1] RYOSUKE KURODA,[1,2] TARO SHOJI,[1,2] HIROTO IWASAKI,[1] TAKAHIRO SUZUKI,[1] AKIRA OYAMADA,[1] MIKI HORII,[1] AYUMI YOKOYAMA,[1] HIROMI NISHIMURA,[1] SANG YANG LEE,[2] MASAHIKO MIWA,[2] MINORU DOITA,[2] MASAHIRO KUROSAKA,[2] AND TAKAYUKI ASAHARA[1,3]*

[1]*Stem Cell Translational Research, Kobe Institute of Biomedical Research and Innovation/RIKEN Center for Developmental Biology, Kobe, Japan*

[2]*Department of Orthopedic Surgery, Kobe University Graduate School of Medicine, Kobe, Japan*

[3]*Department of Regenerative Medicine and Research, Tokai University School of Medicine, Kanagawa, Japan*

We recently reported that systemic administration of peripheral blood (PB) CD34+ cells, an endothelial progenitor cell (EPC)-enriched population, contributed to fracture healing via vasculogenesis/angiogenesis. However, pathophysiological role of EPCs in fracture healing process has not been fully clarified. Therefore, we investigated the hypothesis whether mobilization and incorporation of bone marrow (BM)-derived EPCs may play a pivotal role in appropriate fracture healing. Serial examinations of Laser doppler perfusion imaging and histological capillary density revealed that neovascularization activity at the fracture site peaked at day 7 post-fracture, the early phase of endochondral ossification. Fluorescence-activated cell sorting (FACS) analysis demonstrated that the frequency of BM cKit+Sca1+Lineage− (Lin−) cells and PB Sca1+Lin− cells, which are EPC-enriched fractions, significantly increased post-fracture. The Sca1+ EPC-derived vasculogenesis at the fracture site was confirmed by double immunohistochemistry for CD31 and Sca1. BM transplantation from transgenic donors expressing LacZ transcriptionally regulated by endothelial cell-specific Tie-2 promoter into wild type also provided direct evidence that EPCs contributing to enhanced neovascularization at the fracture site were specifically derived from BM. Animal model of systemic administration of PB Sca1+Lin− Green Fluorescent Protein (GFP)+ cells further confirmed incorporation of the mobilized EPCs into the fracture site for fracture healing. These findings indicate that fracture may induce mobilization of EPCs from BM to PB and recruitment of the mobilized EPCs into fracture sites, thereby augment neovascularization during the process of bone healing. EPCs may play an essential role in fracture healing by promoting a favorable environment through neovascularization in damaged skeletal tissue.

J. Cell. Physiol. 215: 234–242, 2008.

In recent years, interest has turned to bone formation as an alternative target for regenerative medicine in an attempt to meet clinical demands. Unlike damaged soft tissue, which is predominantly repaired through the production of fibrous scar tissue at the site of the injury, bone defects heal by forming new bone that is indistinguishable from uninjured bone tissue. Although bone repair is a rapid and efficient process with callus formation which bridges the fracture gap, a significant proportion (5–10%) of fractures fail to heal and result in delayed unions or persistent non-unions (Marsh, 1998; Rodriguez-Merchan and Forriol, 2004). Among the various causes of fracture non-union, inappropriate neoangiogenesis is considered to be a crucial factor in failed bone formation and remodeling (Harper and Kalgsbrun, 1999; Colnot and Helms, 2001; Karsenty and Wagner, 2002). However, the pathophysiological role of neovascularization in the fracture healing process is not fully understood. As current therapies are still mostly ineffective, a more in-depth analysis of the cellular and molecular mechanisms underlying neovascularization in fracture healing will offer novel opportunities for the development of new therapies for patients with a high risk of delayed- or non-union type fractures.

We have clarified that tissue ischemia and cytokine mobilize endothelial progenitor cells (EPCs) from bone marrow (BM) to peripheral blood (PB), and mobilized EPCs specifically home to sites of nascent neovascularization and differentiate into mature endothelial cells (ECs) (vasculogenesis) in hindlimb ischemic animal model (Asahara et al., 1997, 1999; Takahashi et al., 1999). In addition, we quite recently reported that mouse Sca1+Lineage− (Lin−) cells, an EPC-enriched fraction (Takahashi et al., 1999; Otani et al., 2002; Rafii and Lyden, 2003), increased in PB in the natural course of fracture healing and that human peripheral blood CD34+ cells, hematopoietic stem cell (HSC)/EPC-enriched population, were recruited to the

T. Matsumoto and Y. Mifune contributed equally to this work.

*Correspondence to: Takayuki Asahara, Stem Cell Translational Research, Kobe Institute of Biomedical Research and Innovation/RIKEN Center for Developmental Biology, 2-2 Minatojima-Minamimachi, Chuo-ku, Kobe 650-0047, Japan.
E-mail: Asa777@aol.com

Received 9 January 2007; Accepted 30 August 2007

DOI: 10.1002/jcp.21309

fracture site following intravenous transplantation, developing a favorable environment for fracture healing by enhancing vasculogenesis and osteogenesis, leading finally to functional recovery from fracture (Matsumoto et al., 2006). Recently, increase of CD34+/AC133+ cells was reported in PB of patients with fracture, suggesting contribution of PB EPCs to bone healing (Laing et al., 2007). However, the kinetics and role of EPCs in the natural course of fracture healing has not been fully clarified. Therefore, we tested the following hypothesis that mobilization and incorporation of BM-derived EPCs may be triggered by fracture and the EPC kinetics may contribute to appropriate fracture healing.

In the present study, it was clarified that Sca1+Lin− cells are mobilized from BM to PB in response to fracture, resulting in enhancement of neovascularization of the tissue at the fracture site and contributing to fracture healing. The current discoveries provide novel insight into the fracture healing, in which EPCs are pivotally involved in the pathophysiological processes.

Materials and Methods

Experimental animals

Male C57BL/6 mice (CLEA Japan Inc., Osaka, Japan) aged 10 weeks were used in this study. Green fluorescent protein (GFP) transgenic mice (GFP-Tg mice; C57BL/6TgN [act EGFP] Osb Y01, CLEA Japan) were used in the cell transplantation study as donor mice. Tie-2 transgenic mice (FVB/N-TgN[TIE2LacZ]182Sato; CLEA Japan) and FVB/N mice (CLEA Japan) were used in BM transplantation (BMT) study. All experimental procedures were conducted in accordance with the Japanese Physiological Society Guidelines for the Care and Use of Laboratory Animals and the study protocol was approved by the Ethics Committee in RIKEN Center for Developmental Biology.

Induction of femoral fracture

All surgical procedures were performed under anesthesia and normal sterile conditions. Anesthesia was performed with ketamine hydrochloride (60 mg/kg) and xylazine hydrochloride (10 mg/kg) administered intraperitoneally. A lateral parapatellar knee incision on the right hindlimb was made to expose the distal femoral condyle. An animal model of femoral fracture was applied using a modification of the method described by Manigrasso and O'Connor (2004). Wedge making by 2 mm with a 27-gauge needle on the interchondyle of the femur was performed and then a 0.5-mm diameter, stainless wire was inserted in a retrograde fashion to avoid significant displacement of the fracture by obtaining well aligned stability in the fracture site. The wire was advanced until its proximal end and positioned stable in the greater trochanter and the distal end was cut close to the articular surface of the knee. A transverse femoral shaft fracture was then created in the right femur of each mouse using a C-shaped instrument applying three-point bending. The wound was then irrigated with 10 cc of sterile saline and skin was closed in layers with 5-0 nylone sutures. Post-operative pain was managed by subcutaneous injection of buprenorphine hydrochloride. Unprotected weight bearing was allowed immediately post-operation.

Radiological assessment

Twenty animals were assigned for radiological observation of the healing process. If the fracture produced was not stable or if deep infection developed, then animals was excluded from the study and replaced with other animals. In total, six mice with comminuted fractures and no mice with infections on radiograph were replaced during the study. Radiographs of the fractured legs were serially taken at weeks 0, 1, 2, 3, and 4 following creation of the fracture. This procedure was done under anesthesia with the animal supine and both limbs fully extended. Fracture union was identified by the presence of bridging callus on two cortices.

Tissue harvesting

Mice were euthanized with an overdose of ketamine and xylazine. Bilateral femurs were harvested and embedded in OCT compound, snap frozen in liquid nitrogen, and stored at −80°C for histochemical staining and immunohistochemistry as described below. Mouse femurs in OCT blocks were sectioned, and 6 μm serial sections were collected on slides followed by fixation with 4.0% paraformaldehyde at 4°C for 5 min and stained immediately.

Histological assessment of bone healing, morphometric evaluation of capillary density and immunofluorescence staining

Five rats were randomly selected from 20 other than radiological study and sacrificed for histological assessment at weeks 0, 1, 2, 3, and 4 (the samples at week 4 were obtained after radiological evaluation). Histological evaluation was performed with toluidine blue staining to address the process of endochondral ossification.

Histochemical staining with fluorescent-conjugated isolectin B4 for mouse EC marker (Vector Laboratories Inc., Burlingame, CA) was performed at weeks 0, 1, 2, 3, and 4, and capillary density was morphometrically evaluated by histological examination of five randomly selected fields of soft tissue sections in peri-fracture site (n = 5 in each group). Capillaries were recognized as tubular structures positive for isolectin B4. DAPI solution was applied for 5 min for nuclear staining.

To detect Sca1+ cell-derived EC differentiation at the fracture site of simple fracture model using wild type mice, double immunohistochemistry was performed 1 and 4 weeks post-fracture with the rat anti-mouse PECAM-1 (CD31) (Biogenesis Inc., Poole, UK) and goat anti-mouse Sca1 (Santa Cruz Biotechnology Inc., Santa Cruz, CA) antibodies (n = 5 in each group). The secondary antibodies for each immunostaining are as follows: FITC-conjugated anti-rat IgG (H + L) (Jackson ImmunoResearch Laboratory Inc., West Grove, PA) for PECAM-1 and Cy3-conjugated anti-goat IgG (H + L) (Jackson) for Sca1 staining. DAPI solution was applied for 5 min for nuclear staining.

All morphometric studies were performed by an experienced examiner who was blinded to each time point.

Physiological evaluation by laser doppler perfusion imaging (LDPI)

LDPI (Moor Instrument, Wilmington, DE) (Wardell et al., 1993; Linden et al., 1995) was used to measure serial blood flow over the course of 4 weeks post-fracture (n = 5 in each group). This examination was performed under anesthesia with the animal supine and both limbs fully extended. Blood flow was assessed by the ratio of flux in the fractured hindlimb with that in the intact (contralateral) side.

Isolation of Lin− cells from BM and PB for fluorescence-activated cell sorting (FACS) analysis

BM cells were obtained by flushing femurs and tibias of 10-week-old mice pre- and 7 days post-fracture with phosphate-buffered saline (PBS) containing 5% fetal calf serum (PBS-FCS) (n = 5 in each group). PB was also aspirated from the hearts of 10-week-old mice pre- and 7 days post-fracture with PBS-FCS (n = 5 in each group). BM and PB mononuclear cells (MNCs) were obtained by density gradient centrifugation at 400g for 20 min with Histopaque-1083 (Sigma-Aldrich Inc., St Louis, MO). The light-density MNCs were collected, washed twice with Dulbecco's PBS supplemented with 2 mM EDTA and counted manually. To deplete mature hematopoietic cells such as T cells, B cells, NK cells, monocytes/macrophages, granulocytes, and erythrocytes from the total MNCs, separation of Lin- cells was performed by staining with a cocktail of biotinylated monoclonal antibodies against the lineage markers [B220/CD45R, clone RA3-6B2; CD11b (Mac-1), clone Mi/70; Gr-1, clone RB6-8C5; Thy1.2, clone 53-2.1; CD3e, clone 145-2C11; CD4, clone RB6-8C5; CD8, clone 53-6.72; and TER 119, clone Ly-76; BD Pharmingen, San Diego, CA] followed by